自由電子雷射的調制器與發光器 (Modulators and radiators for Seeded FEL)
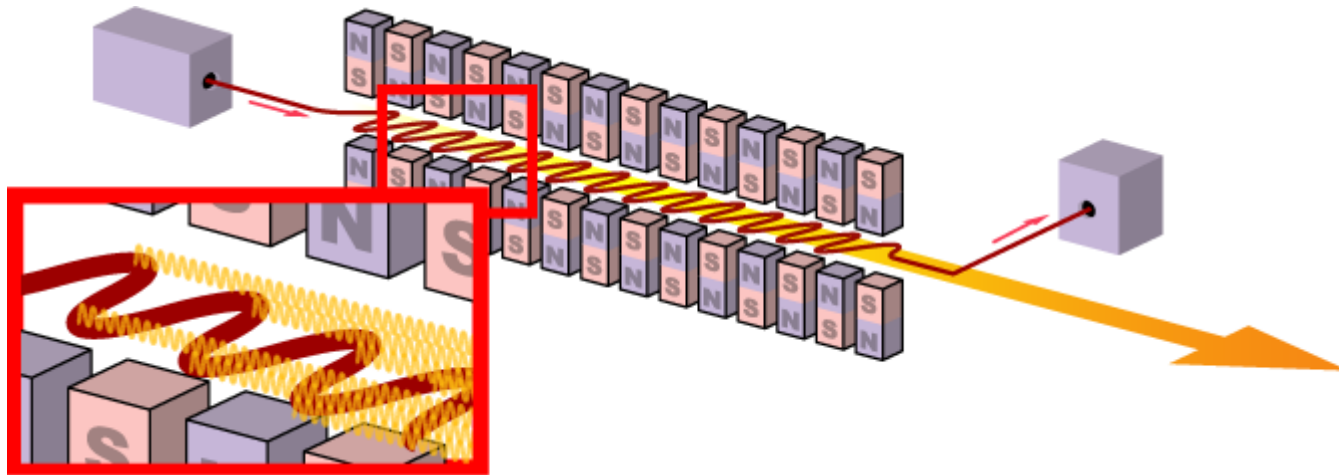
Ching-Shiang Hwang

（黃清鄉）

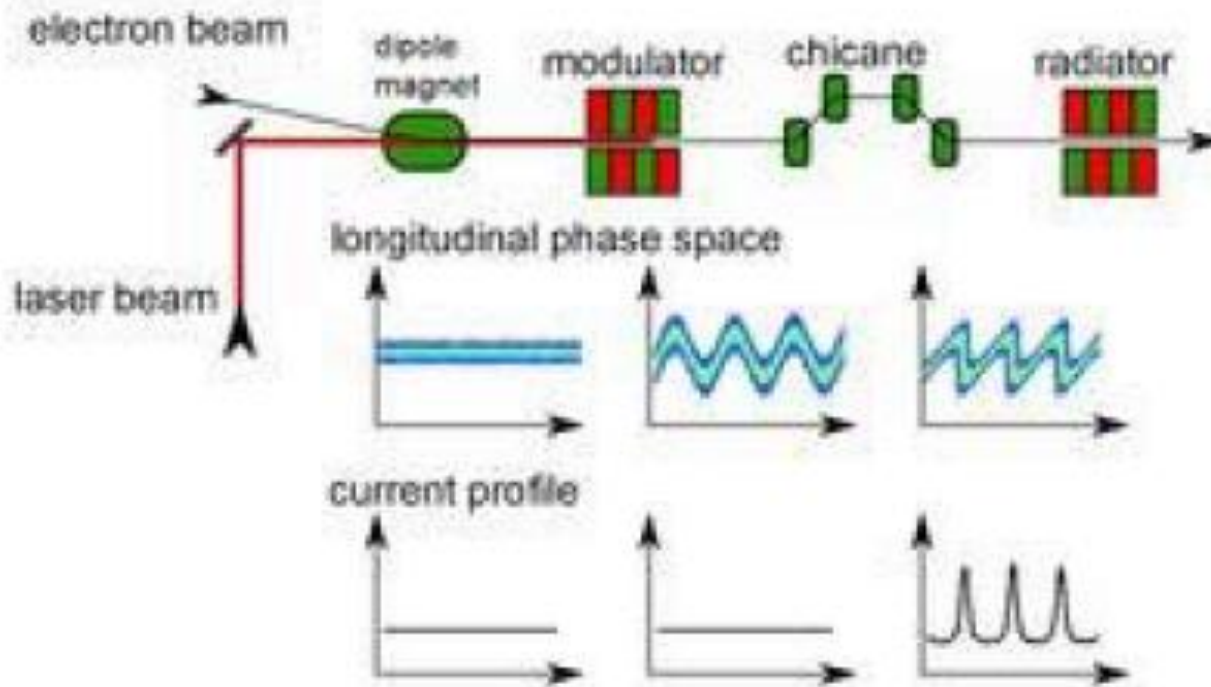**cshwang@alumni.nsrrc.org.tw**

July 4th, 2023 13:00-15:00

Modulator and Radiator (ID) for FEL

Radiator

Modulator

electron beam

dipole magnet modulator chicane radiator
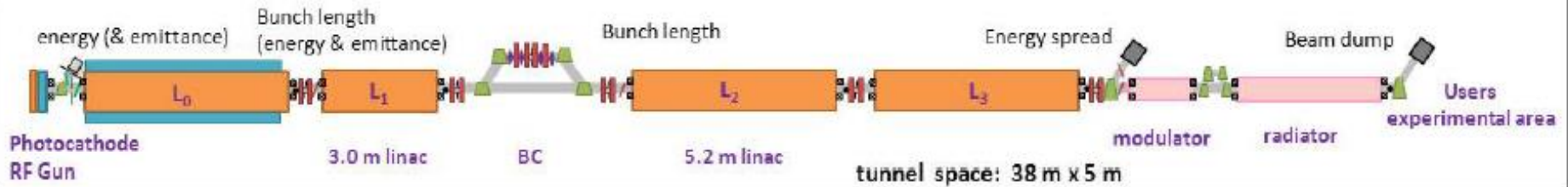
longitudinal phase space

laser beam

current profile

Outline

- **Application of Insertion Devices (ID)**
- **Introduction of ID**
  - **Wiggler (增頻磁鐵) & Undulator (聚頻磁鐵)**
  - **Development history**
- **Spectrum features & calculation**
  - **Flux, Flux density, Brilliance**
  - **Power, power density**
- **Example of the ID spectrum**
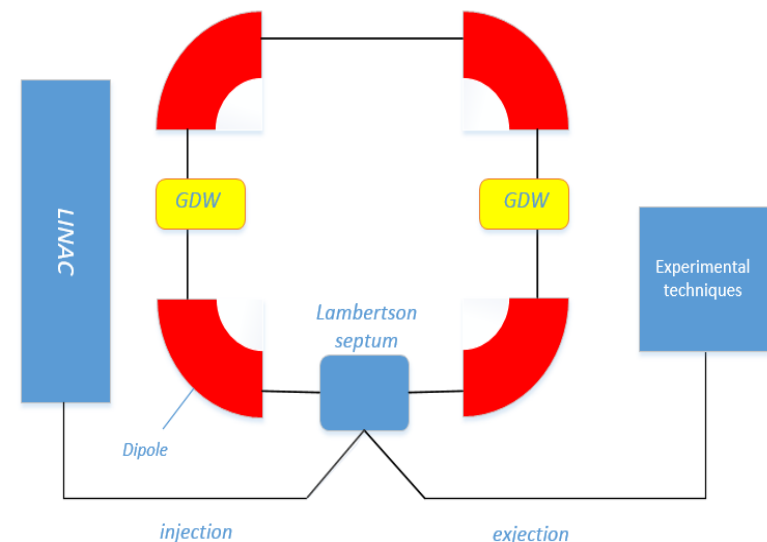- **How to design and shimming ID**

2

Application of Insertion Device (ID)

(1) Modulator or Radiator in FEL structure
(2) Main light source in storage ring (SR) structure
(3) Robinson wiggler to reduce emittance of SR
(4) Gradient damping wiggler to vary damping partition number & momentum compaction factor of SR

3
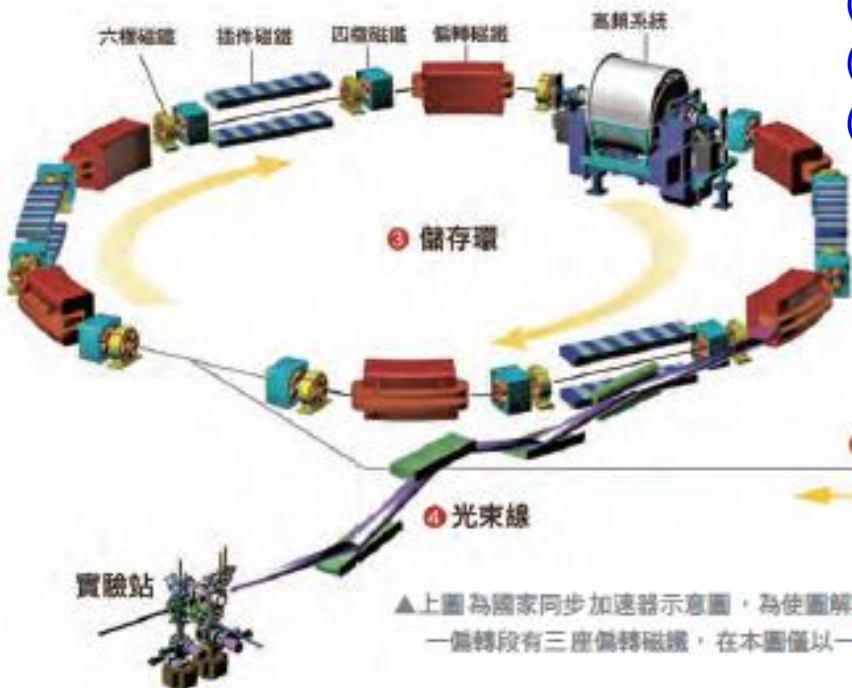
Introduction & history

- Insertion devices include the wigglers（增頻磁鐵）and undulators（聚頻磁鐵）that are magnetic devices producing a specially periodic field variation.

- They are all placed in the straight sections of storage ring.

- Wiggler spectrum at higher photon energies is smooth, similar to that of a bending magnet. The radiation intensity can be much higher as much as increased numbers of poles and higher magnetic field generate radiation with a higher critical energy.

- When the use of periodic magnets in a regime in which interference effects is coherent, and then the device is called "undulator".

- The main radiation features of insertion devices are (1) higher photon energy, (2) higher flux and brightness, (3) different polarization characteristics.

- The theory behind undulators was developed by Vitaly Ginzburg in the USSR.

- First undulator was installed in a linac at Stanford, using it to generate millimetre wave radiation through to visible light in 1953.

- First wiggler (undulator) installed in storage ring at SSRL (BINP) around at 1979s.

- Superconducting wavelength shifter: are currently operating in several synchrotron radiation facilities: ESRF, UVSOR, PF and CAMAD (USA), NSRRC begin early 1980.

- EPU (APPLEII) solve the experimental problem of circular polarization light at 1994.

- Superconducting wigglers: are currently used in MAXLab, NSRRC, Diamond, ALBA,...

- In-vacuum undulator: are popular used in the new 3th generation light source.

- Cryogenic permanent-magnet undulator: ESRF & SPring8, Diamond, Soleil, NSRRC.

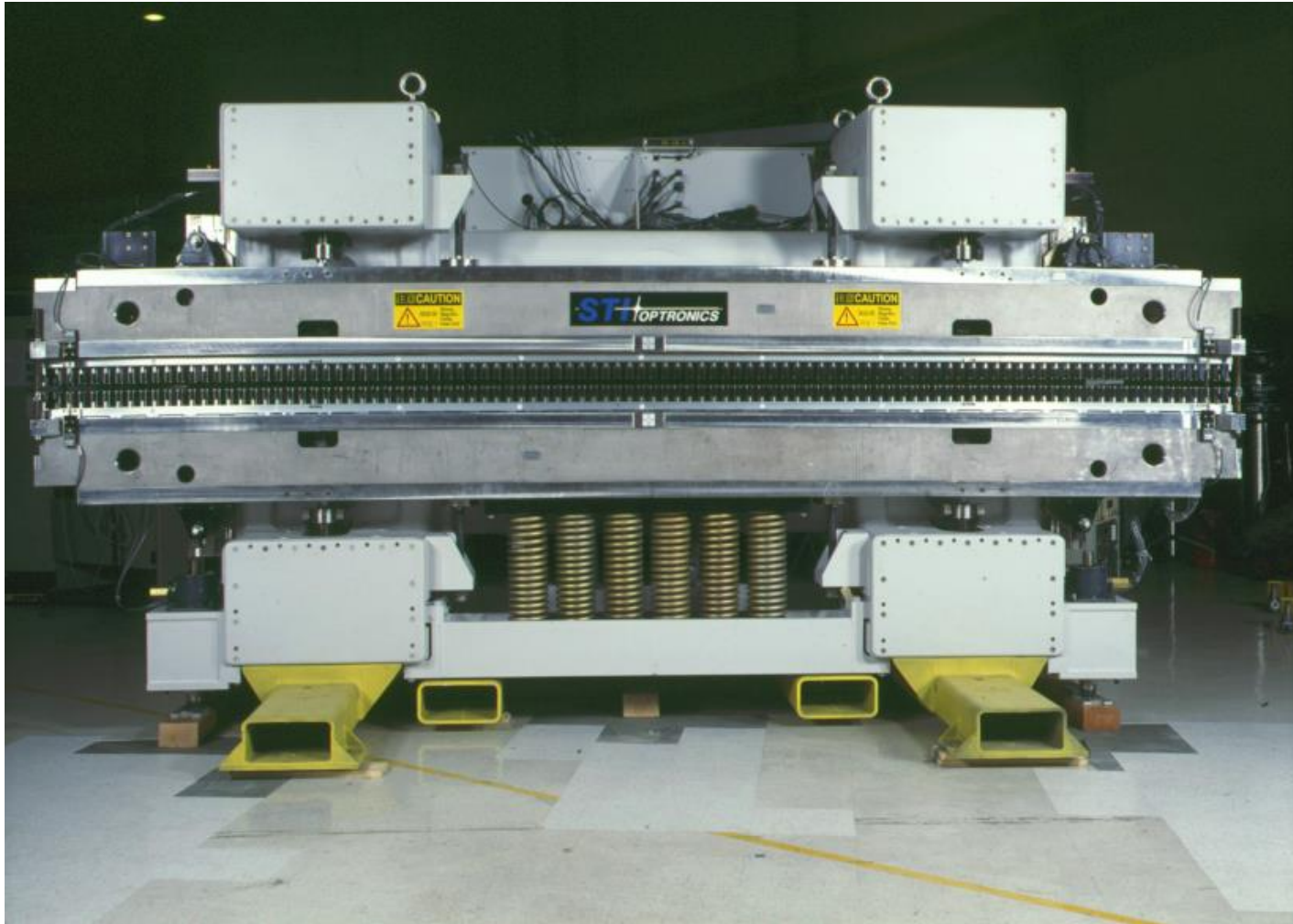- Superconducting Undulator: In developing in NSRRC, ANKA, BASSY II, APS.

電磁波家族成員

➢ 十九世紀中葉，馬克斯威爾（Maxwell）將電磁學理論架構整理，建立了電磁波理論(1865)。電磁波以光速傳播，而『光』是一種電磁波。

➢ 「同步加速器光源」為一連續波段的電磁波，涵蓋紅外光、可見光、紫外光、軟X光、硬X光等波段。
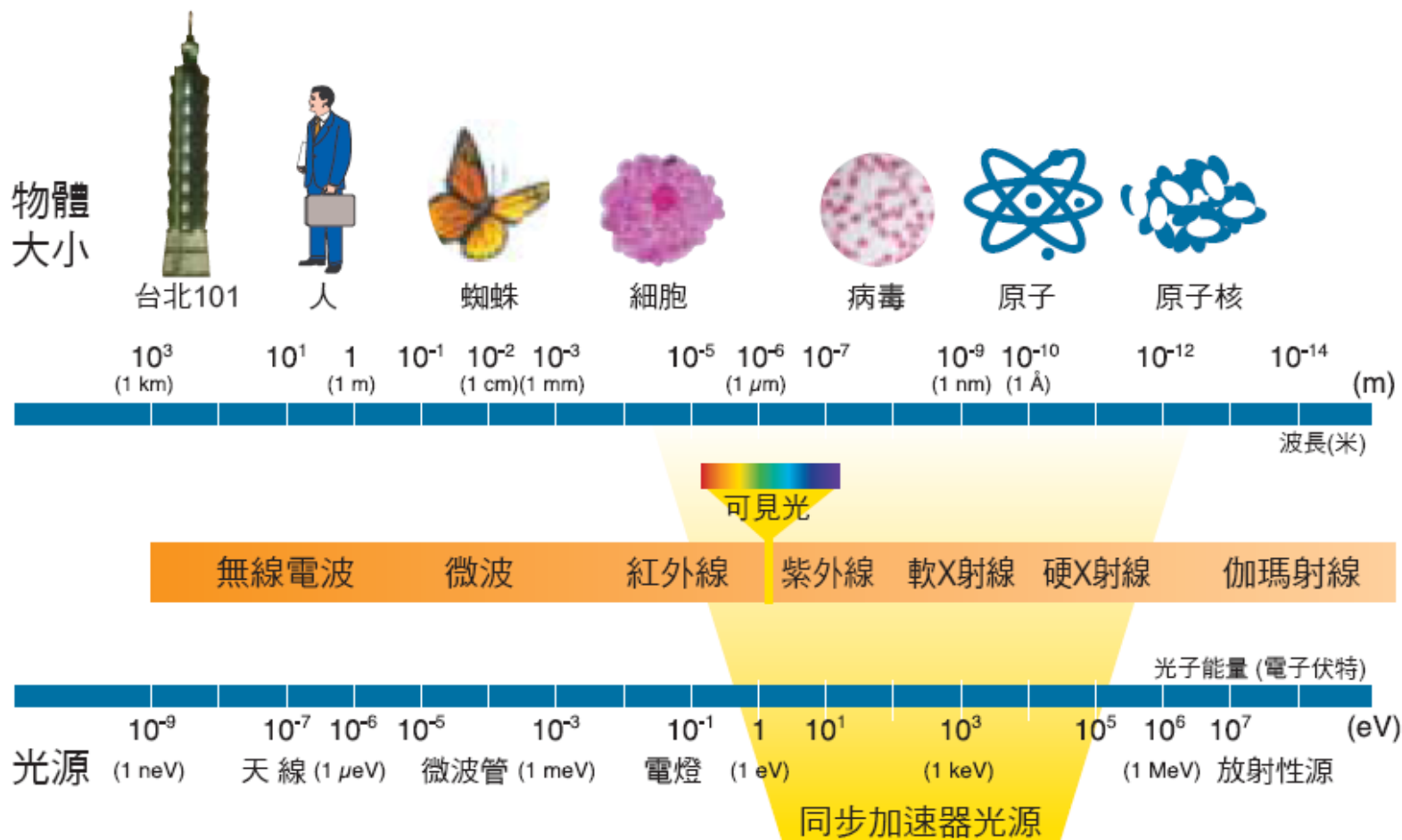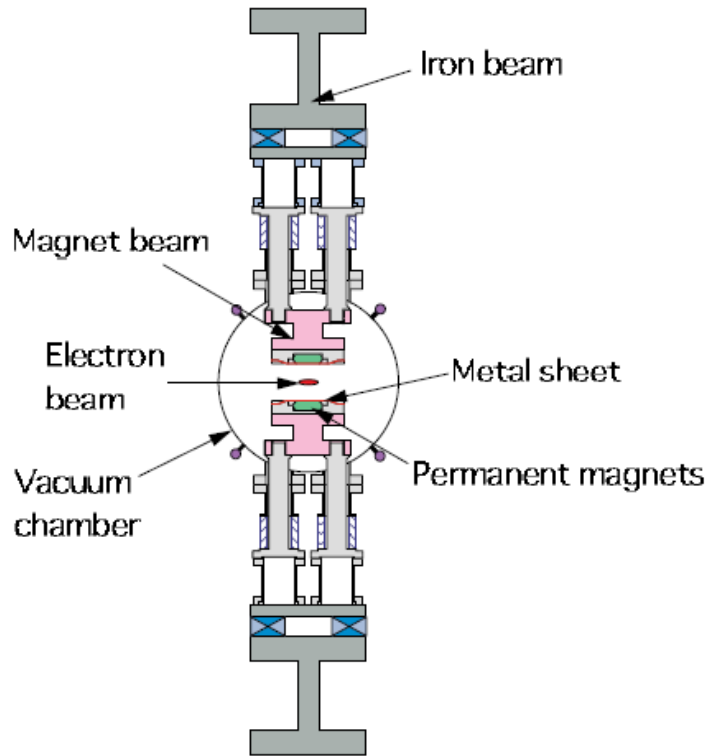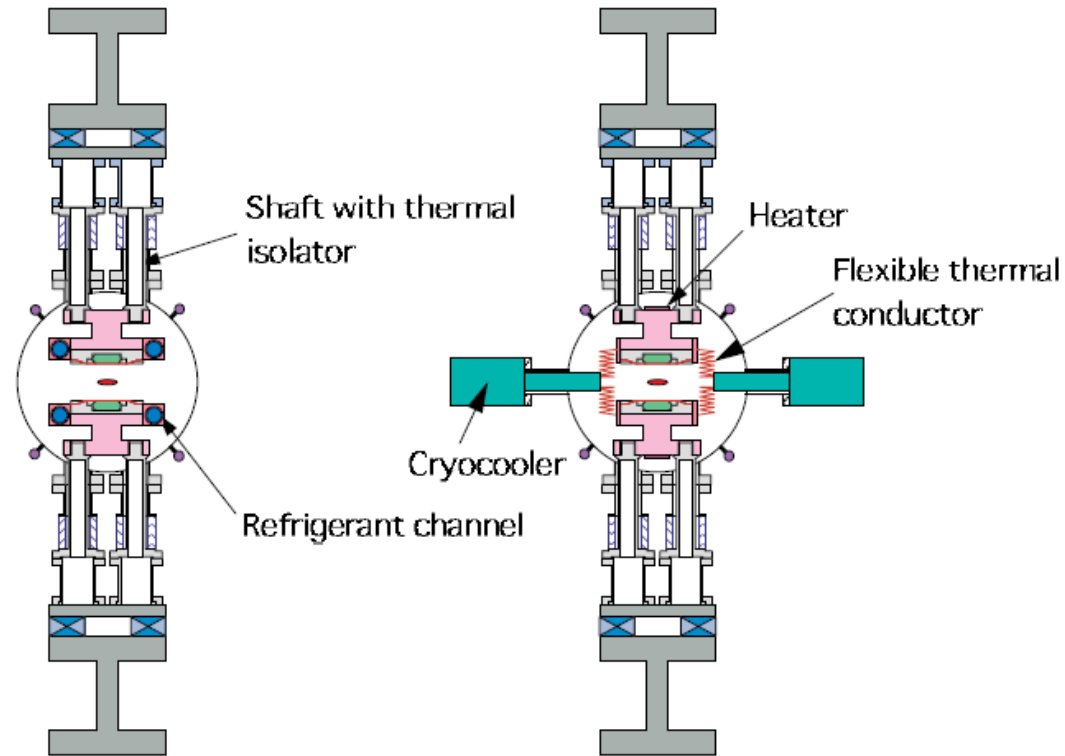
真空外聚頻磁鐵

In-vacuum (IU) & cryogenic undulator (CU)

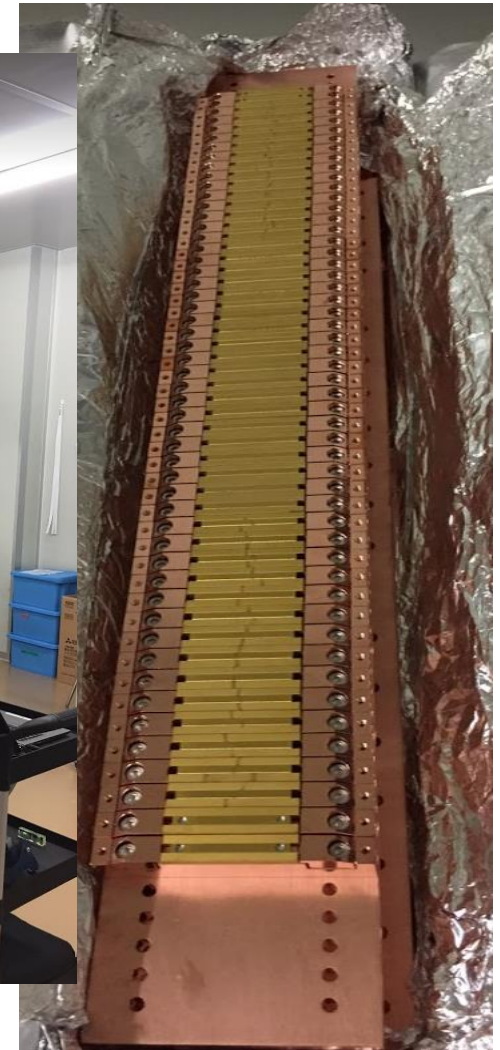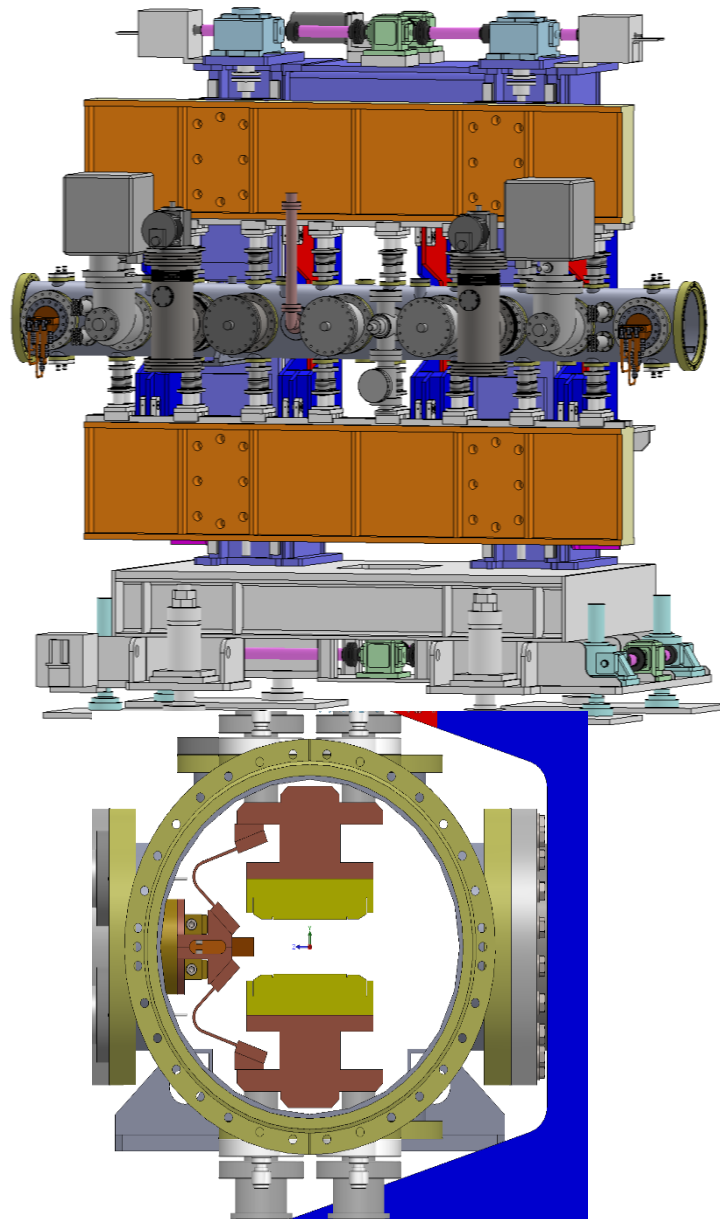IU @Room Temperature   CU Below 77 K   真空內聚頻磁鐵

> The cooling method of CU is (1) liquid nitrogen cryogenic system or (2) the cryocooler.
> The cooling method will depend on numbers of CU.

T. Hara et al., "Insertion Devices of Next Generation", Proceedings of APAC 2004
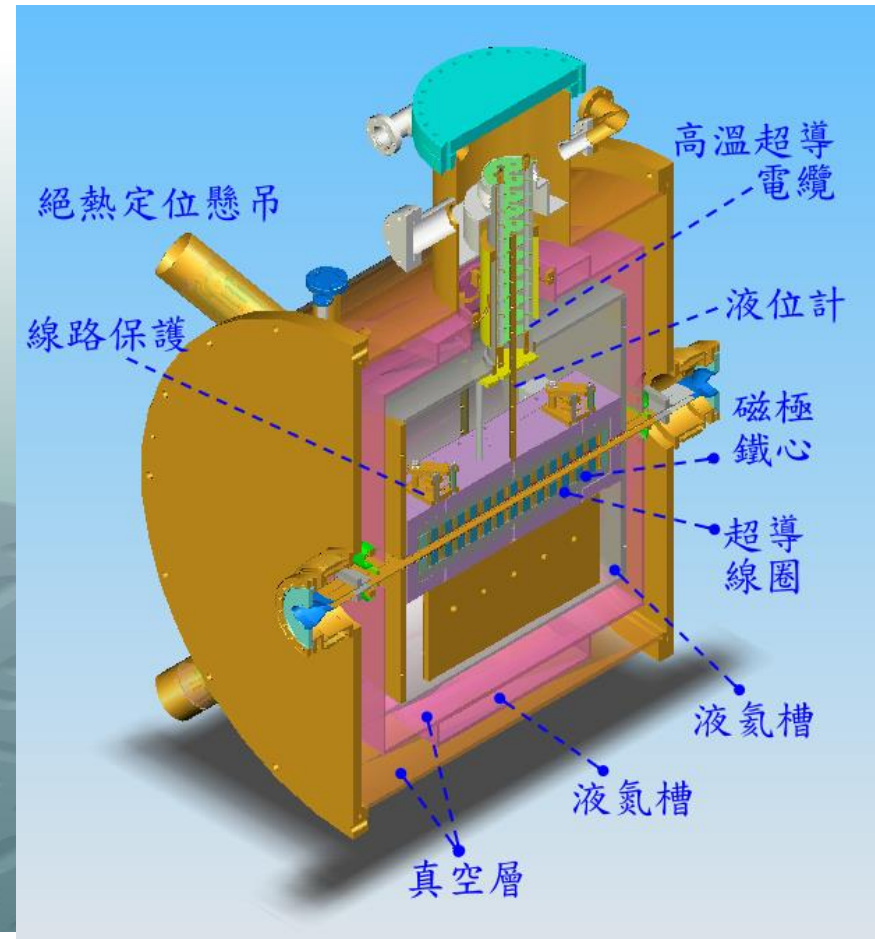
Cryogenic undulator (CU15)

- ◆ 0.6 m long prototype testing
- ◆ 2 m long CU15 will be finished before June 2019
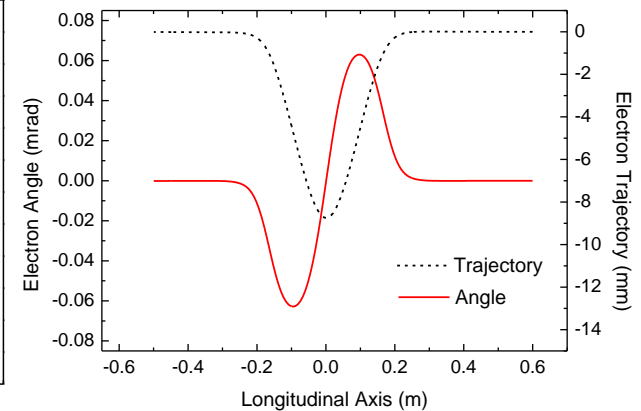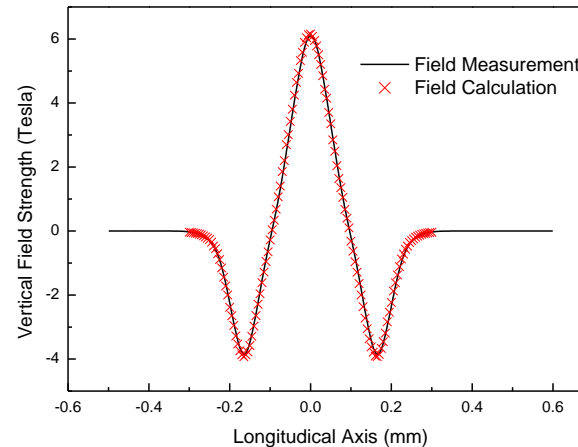- ◆ 200 W CH-110 cryocooler at 77K

絕熱定位懸吊

線路保護

高溫超導電纜

液位計

磁極鐵心

超導線圈

液氦槽

液氮槽

真空層

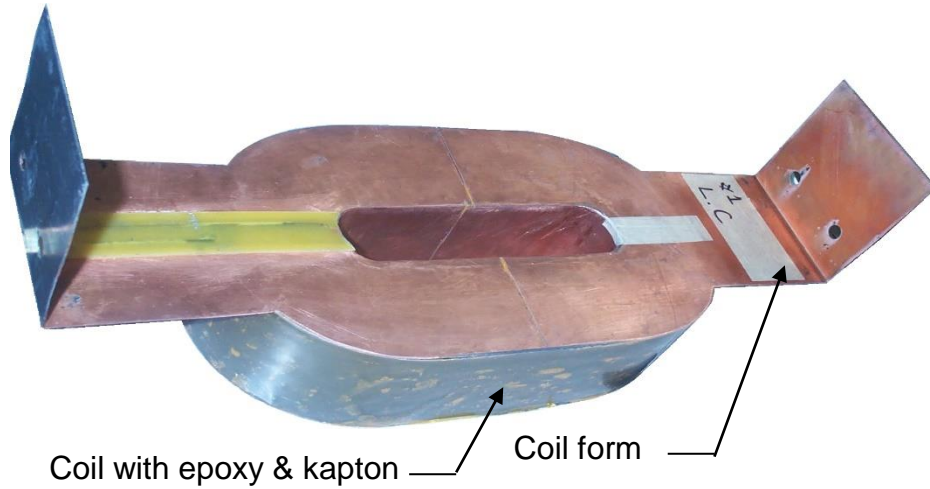# Superconducting wavelength shifter

Coil with epoxy & kapton — Coil form

Alignment pin
Iron
pole
Gap separation
Lower Al block

Survey pinhole
Return yoke
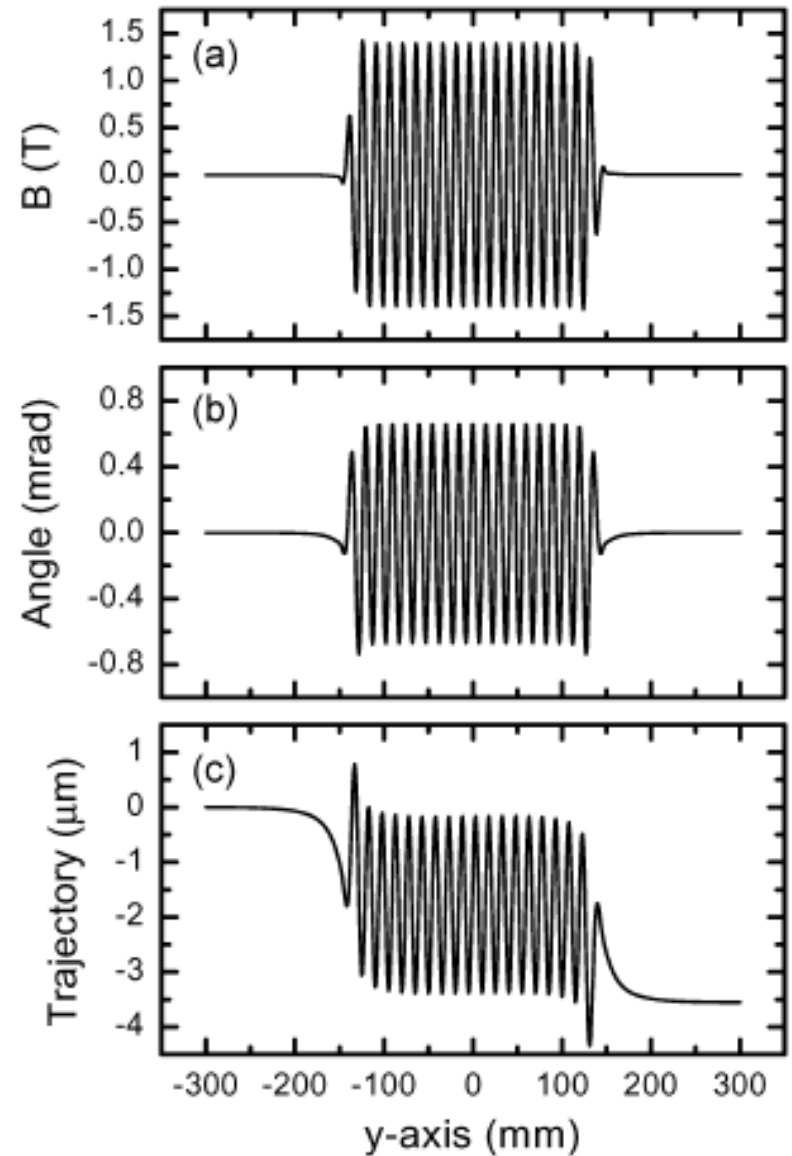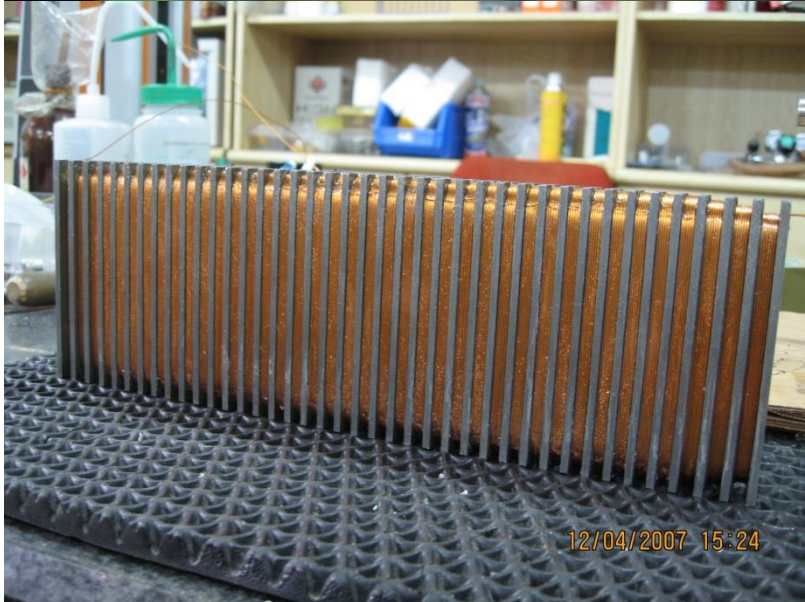Superconducting wire
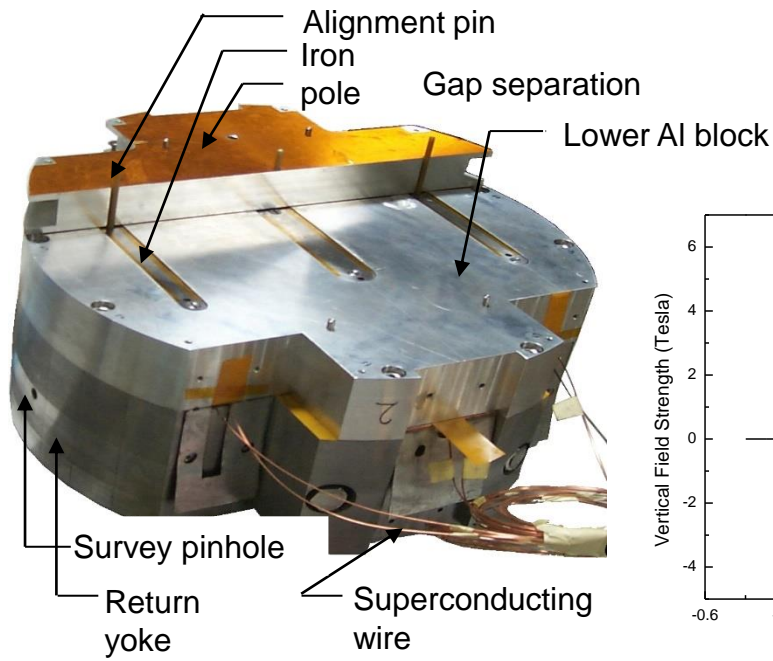
Superconducting undulator (SU15)

產生各種偏振的光－橢圓偏振聚頻磁鐵
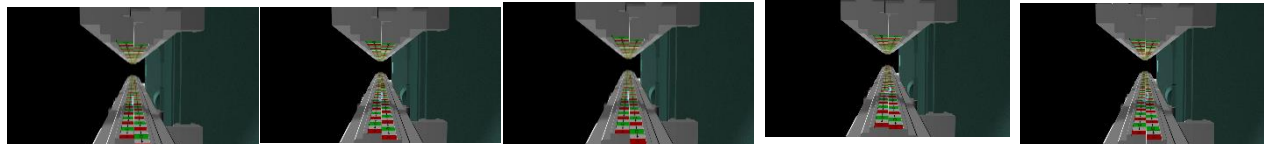
EPU56
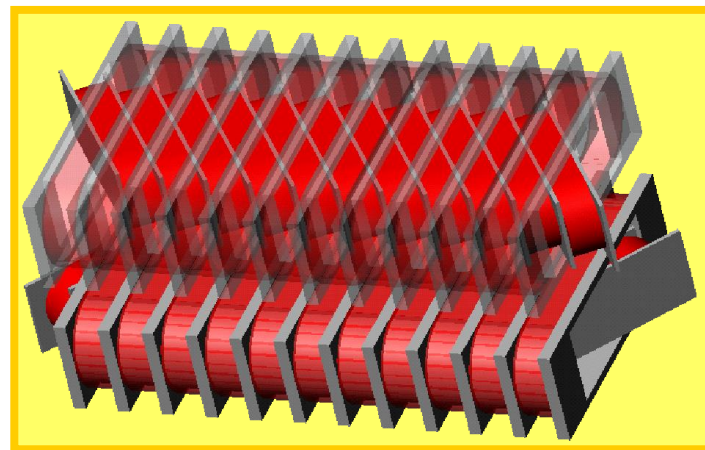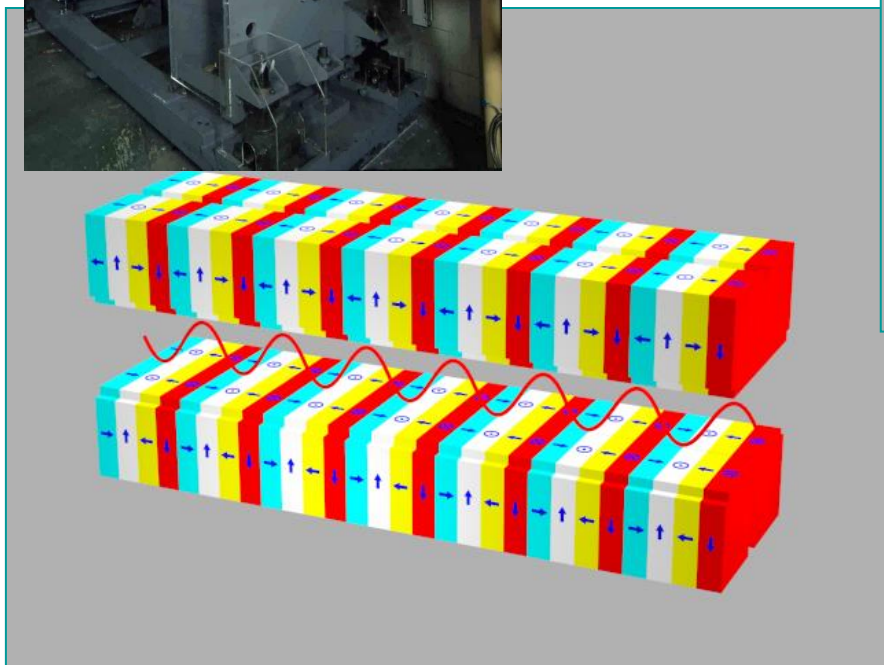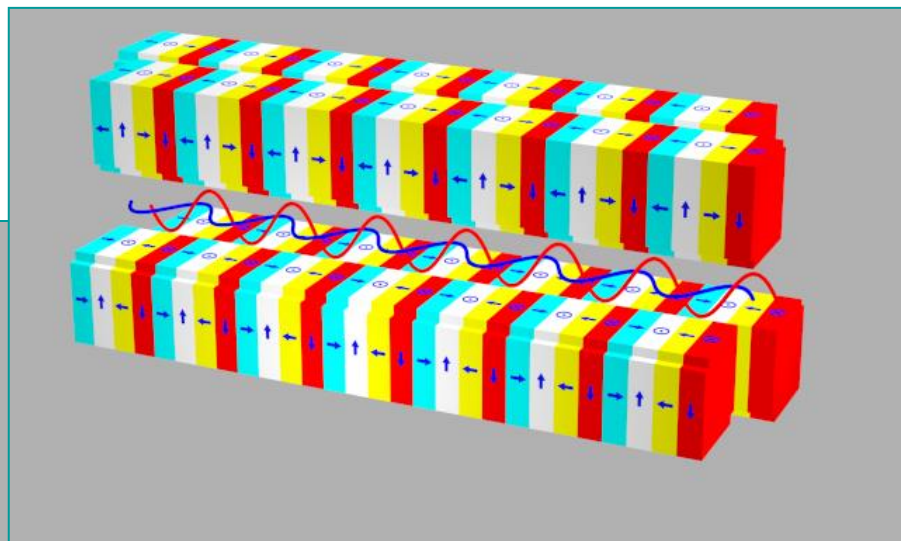
超導橢圓偏振聚頻磁鐵

Staggered Undulator with YBCO Bulks

Staggered magnet array structure
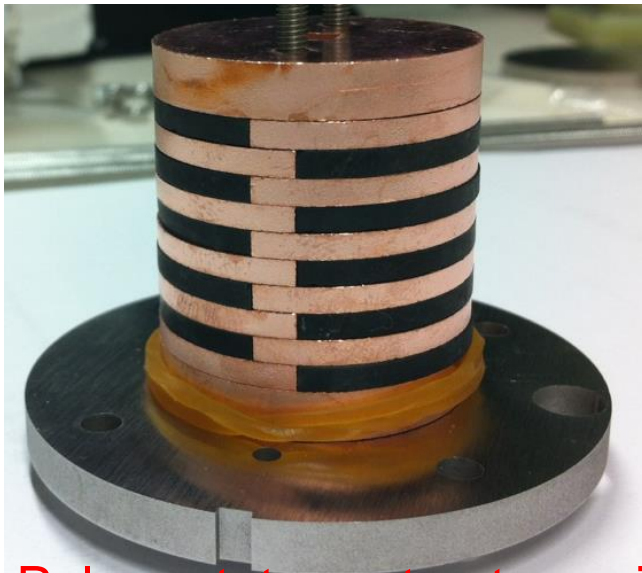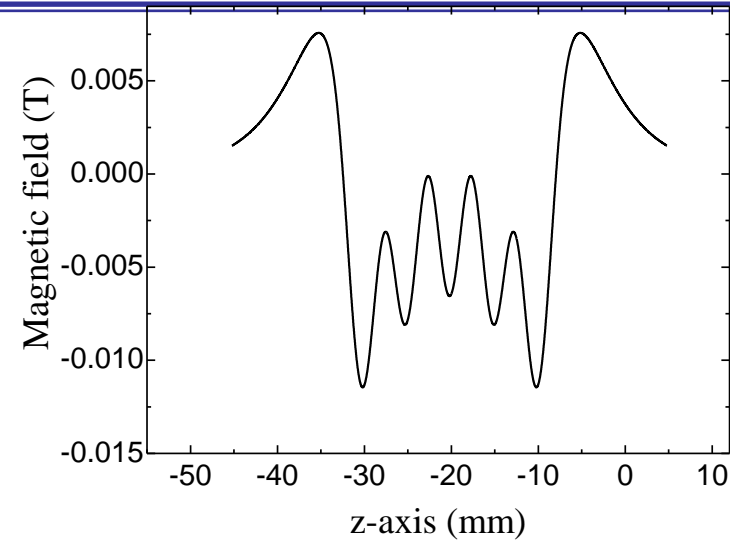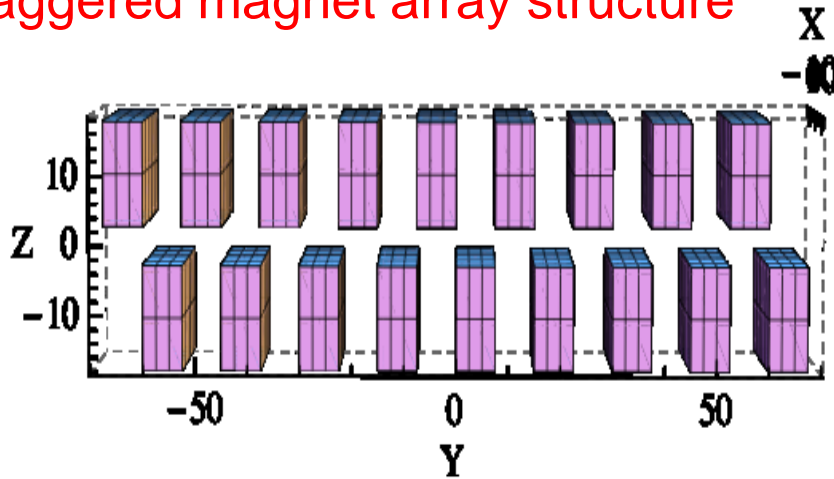
type	Stagger structure
Period length	5mm
# of period	5
gap	4.2mm
total length	25mm
Current density @ 77K	66 A/mm^2

➢ 10 Pole prototype structure without end pole optimization & using Field Cooling method.

➢ The magnet flux density will depend on the trapped field of YBCO bulks.

Synchrotron accelerator light source- Insertion Devices

一、聚頻磁鐵:聚集同一頻率的光使之光量亮增加

二、增頻磁鐵:提昇較高頻率光的光通量

三、移頻磁鐵:提昇光的頻率至較高能量區

電子由此進入磁場

正(北)極

負(南)極

電子團

U90聚頻磁鐵

Halback structure arrays

同步加速器光源

One Sided Flux Sheet

One Sided Flux Sheet

e- Source
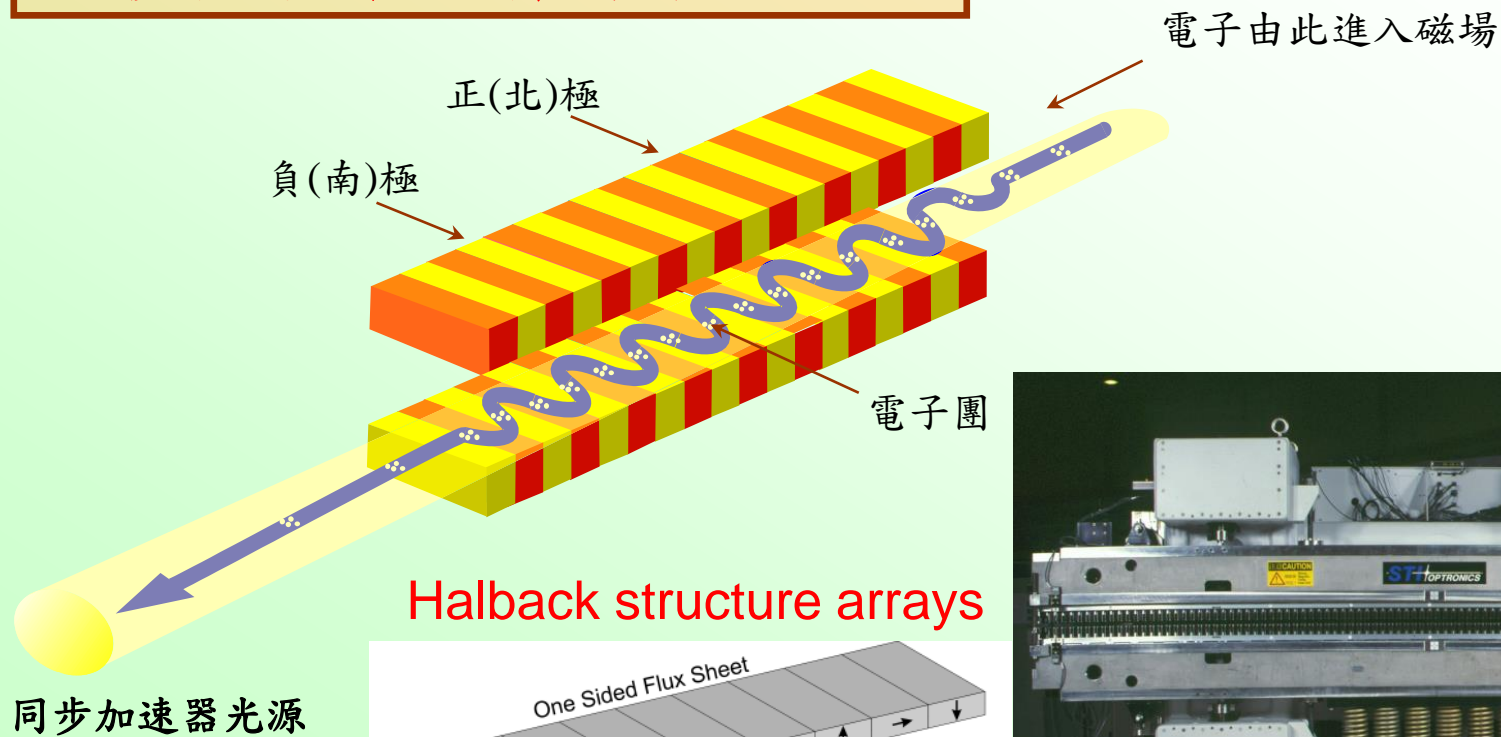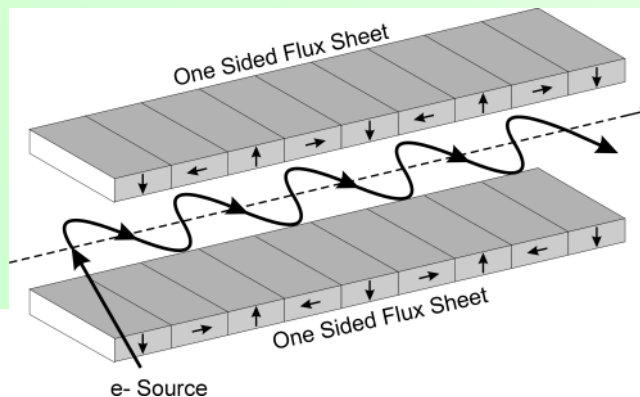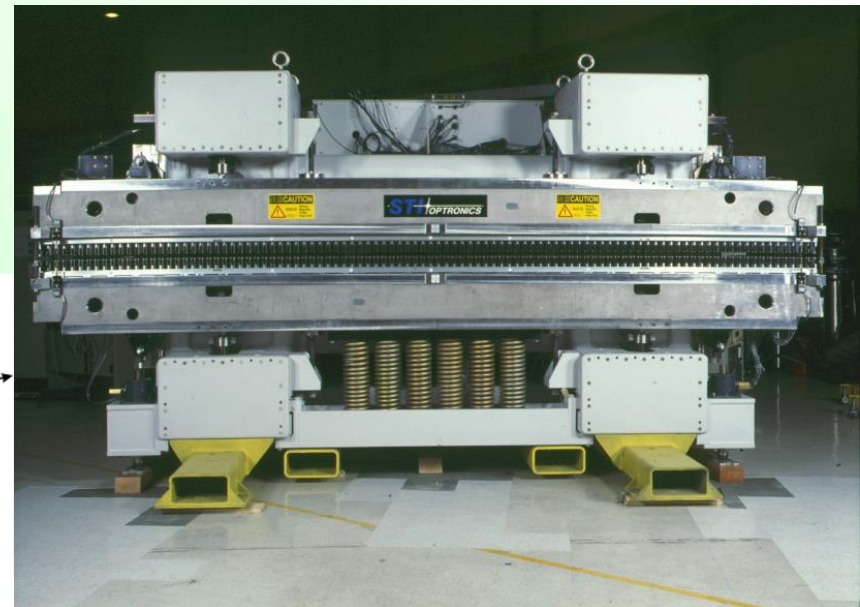
Different features in the insertion devices

Type	Electron Orbit	Electromagnetic field	Spectrum

K<<1
偏向角<< γ_{-1}
Undulator

K~1
偏向角~ γ_{-1}
Undulator

K>>1
偏向角>> γ_{-1}
Wiggler

$$K = \frac{eB_o\lambda_o}{2\pi mc} = 0.934 B_o[T]\lambda_o[cm]$$

15

bending magnet   wiggler   undulator
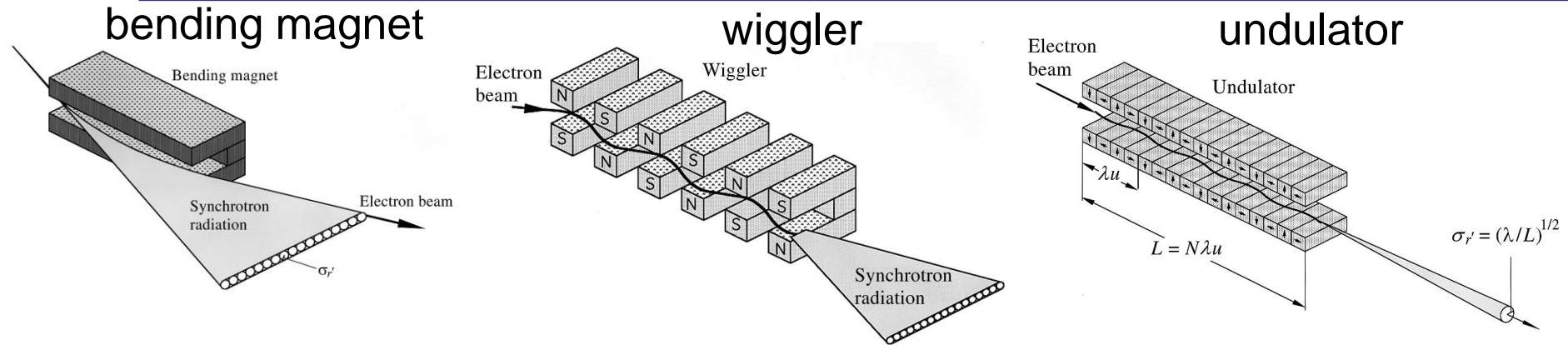
The synchrotron radiation emitted from (a) bending magnet, (b) wiggler, (c) undulator.

◆ The synchrotron radiation emitted from an electron beam which was bent in a spatially periodic sinusoidal field in an insertion device.

◆ An electron beam traveling in a curved path (Bending magnet) at nearly the speed of light emits photons into a narrow cone of natural emission angle $\cong \gamma^{-1}$.

◆ For the wiggler, the horizontal radiation cone become is $k\gamma^{-1}$ and the vertical cone is the same as that of the dipole magnet.

◆ For the undulator, the radiation cone in horizontal and vertical are all closed to be γ^{-1}.

16

Synchrotron Radiation from Insertion Devices
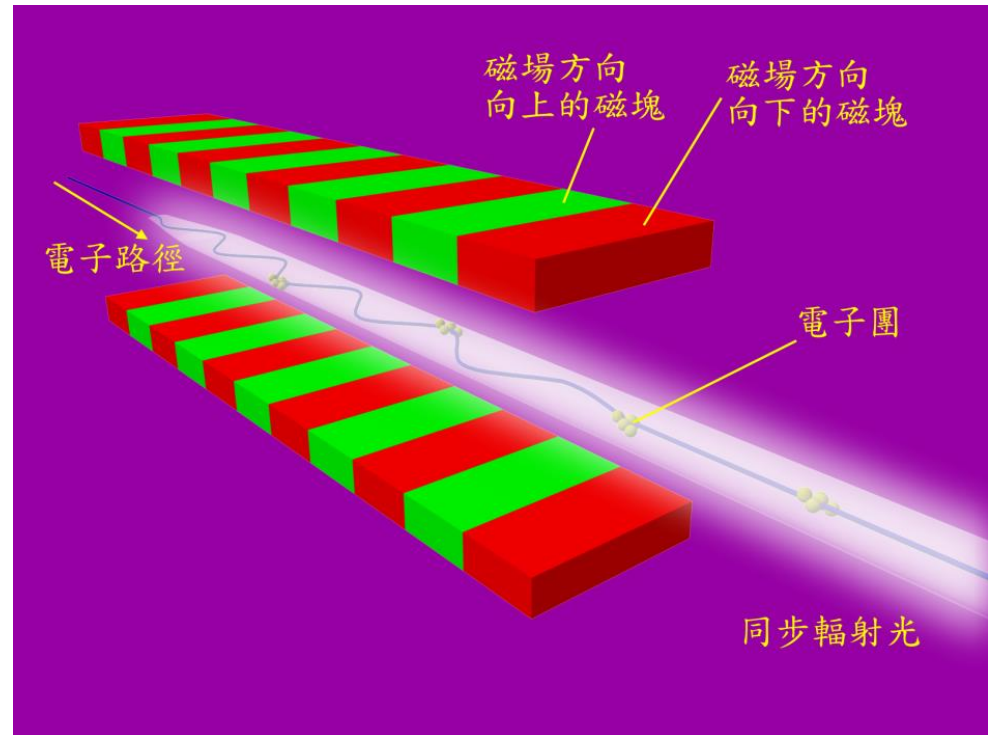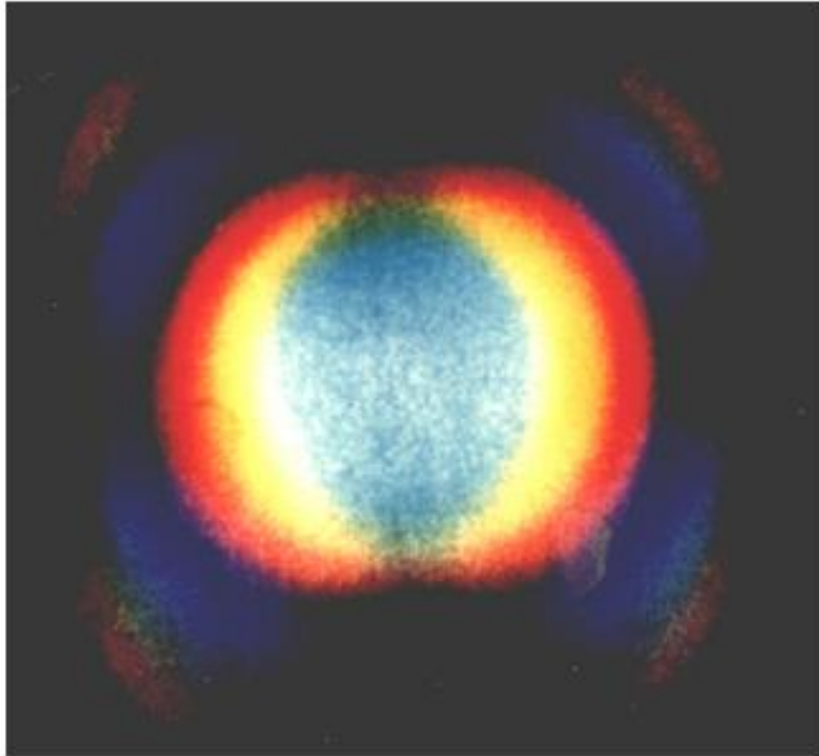
$$\lambda_p = \frac{\lambda_u}{2\gamma^2}\left(1 + \frac{K^2}{2} + \gamma^2\left(\theta^2 + \psi^2\right)\right)$$

$$K = \frac{eB_o\lambda_o}{2\pi mc} = 0.934 B_o[T]\lambda_o[cm]$$

17

Spectrum of bending and insertion devices

Synchrotron Radiation from Insertion Devices

Spatial flux density

Kx=Ky

Ky

E1st

E2nd

E3rd

E5th
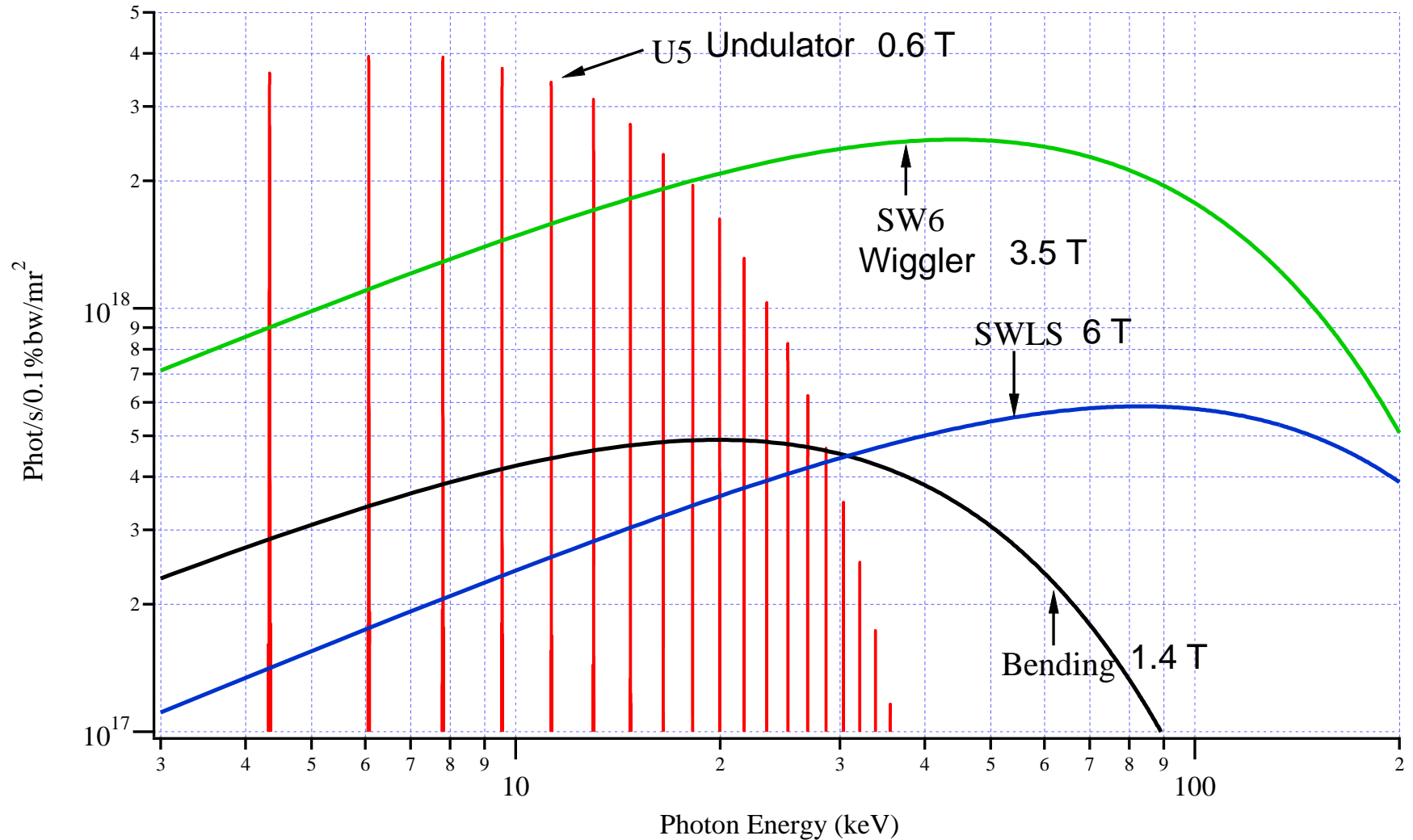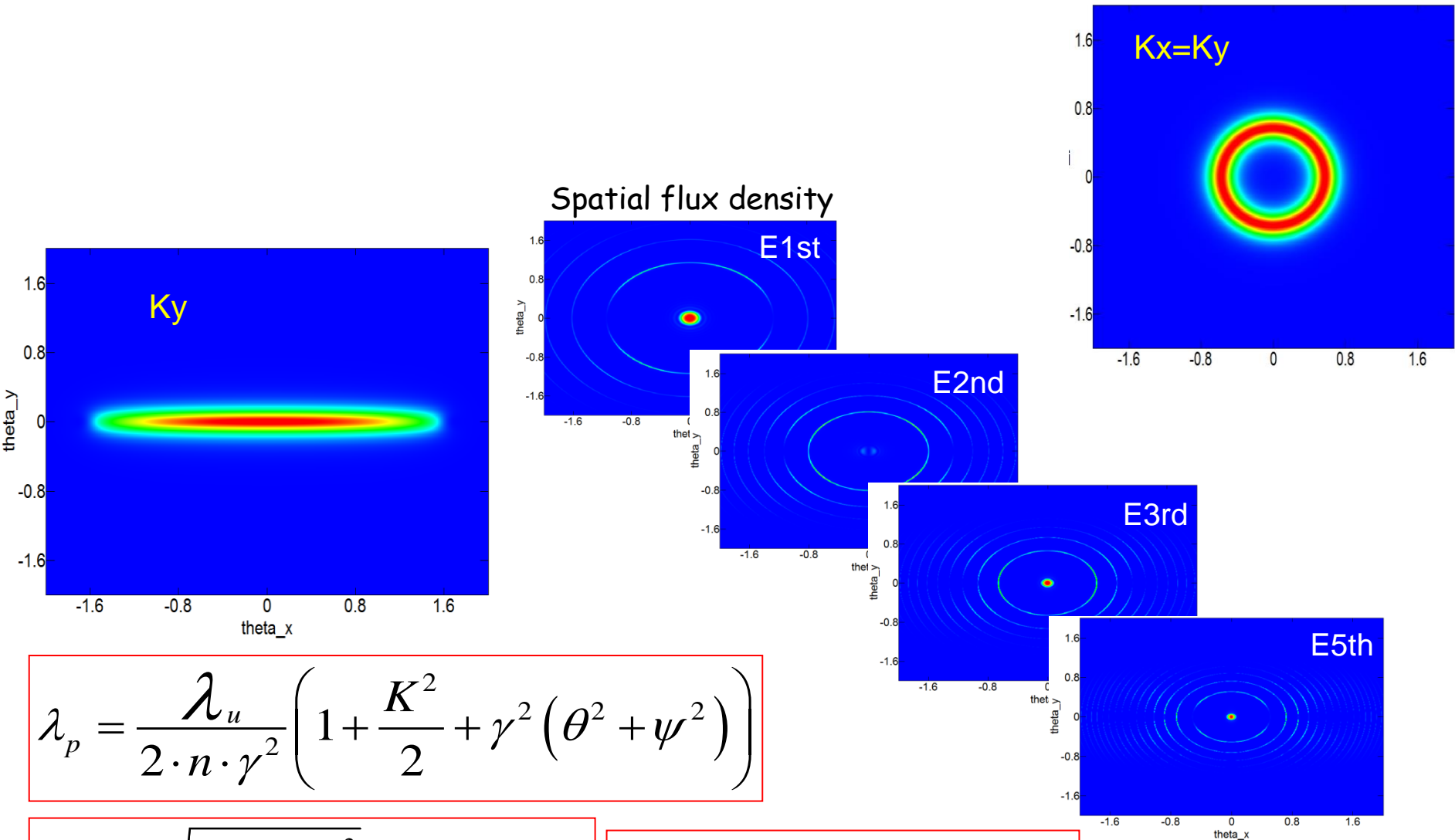
$$\lambda_p = \frac{\lambda_u}{2 \cdot n \cdot \gamma^2}\left(1 + \frac{K^2}{2} + \gamma^2\left(\theta^2 + \psi^2\right)\right)$$

$$\theta_{n,l} = \frac{1}{\gamma}\sqrt{\frac{l}{n}\left(1 + \frac{K^2}{2}\right)}, (l = 1, 2, 3...)$$

$$K = \frac{eB_o\lambda_o}{2\pi mc} = 0.934 B_o[T]\lambda_o[cm]$$

19

光譜比較

Diamond · ALS · SRS · X Ray Tube · Sun · 60W Light Bulb · Candle

Brightness (photons / sec / mm² / mrad² / 0.1% BW)

10^{20}, 10^{19}, 10^{18}, 10^{17}, 10^{16}, 10^{15}, 10^{14}, 10^{13}, 10^{12}, 10^{11}, 10^{10}, 10^{9}, 10^{8}, 10^{7}, 10^{6}, 10^{5}, 10^{4}, 10^{3}, 10^{2}

NSRRC

ESRF-EBS (2020) · ESRF (2014) · Third generation · ESRF (1994) · Second generation · First generation · X-ray tubes

Brilliance (photons/s/mm²/mrad²/0.1%BW)

10^{24}, 10^{23}, 10^{22}, 10^{21}, 10^{20}, 10^{19}, 10^{18}, 10^{17}, 10^{16}, 10^{15}, 10^{14}, 10^{13}, 10^{12}, 10^{11}, 10^{10}, 10^{9}, 10^{8}, 10^{7}, 10^{6}

1900 1920 1940 1960 1980 2000 2020
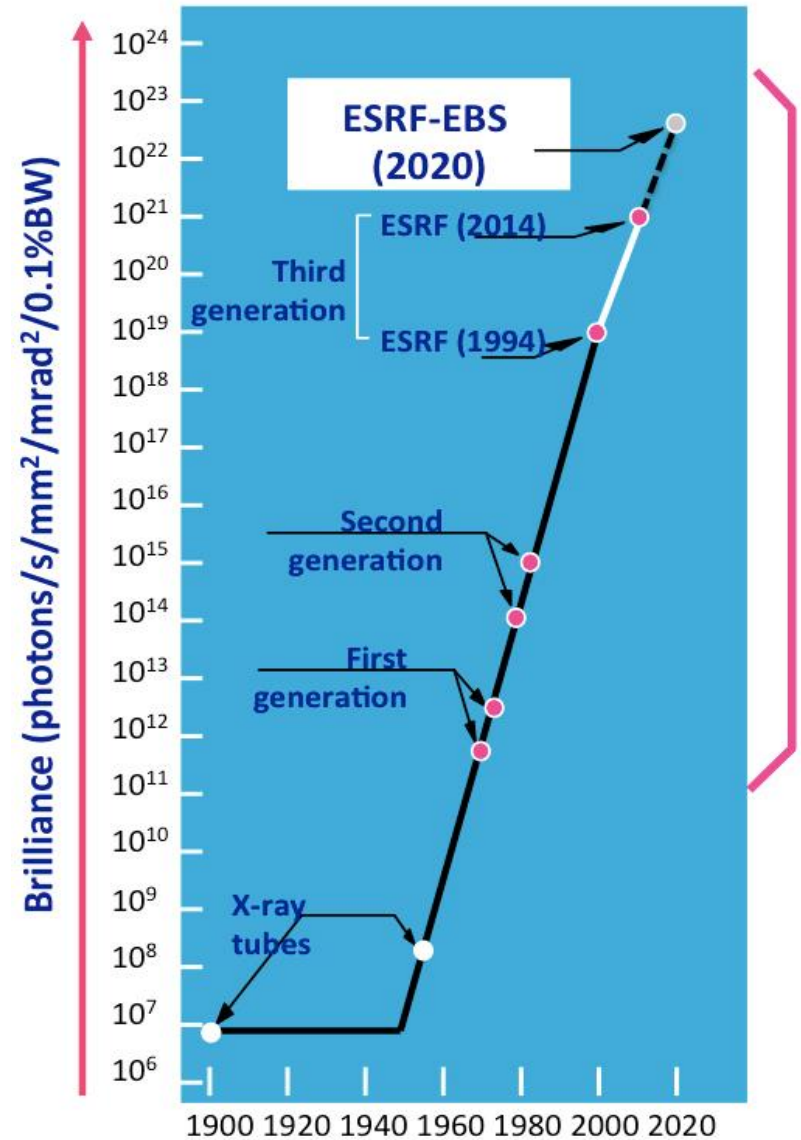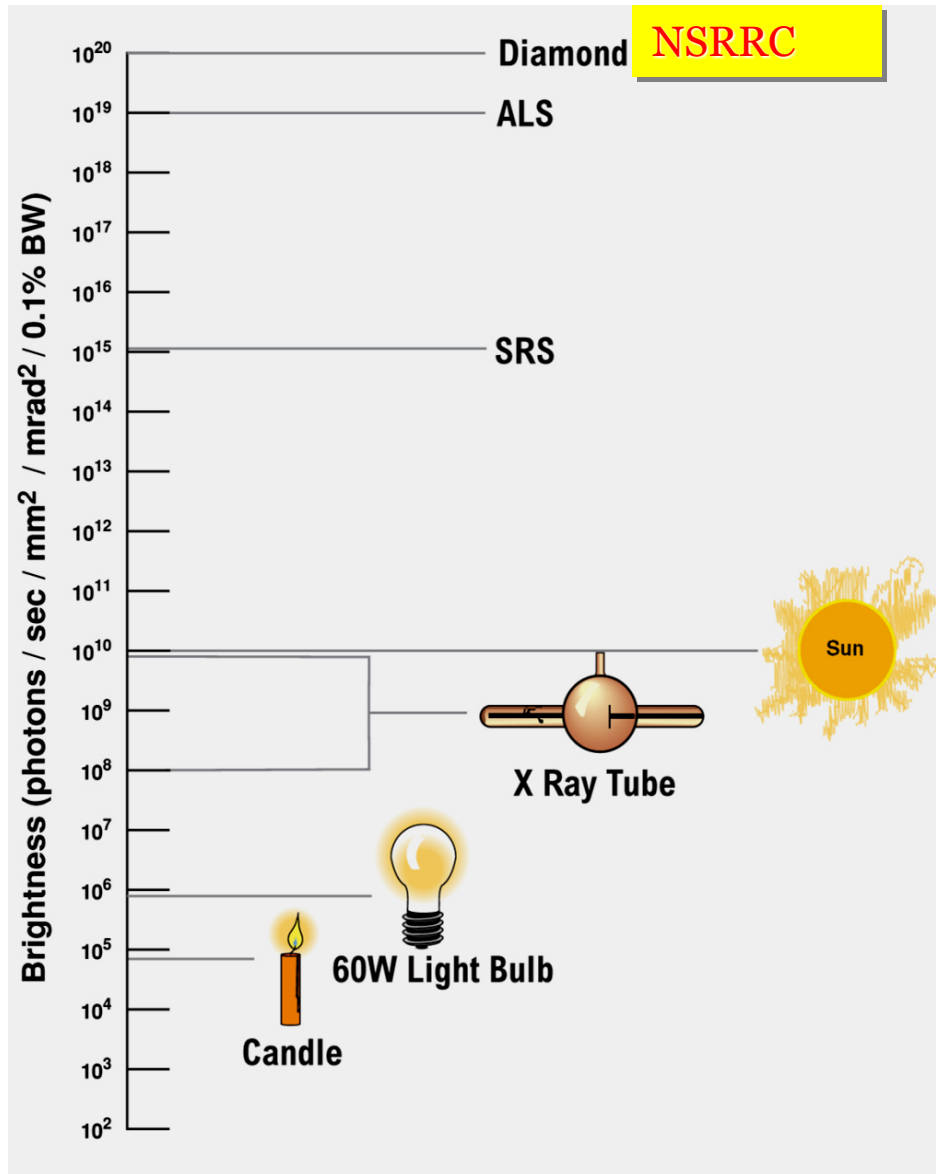
$$B_y(z) = B_0 \cos k_{\mathrm{p}} z \qquad \text{this is what we want}$$

Maxwell tells us what we can get! $B_y(y, z) = B_0\, b(y) \cos k_{\mathrm{p}} z$

$$\nabla \times \mathbf{B} = 0 \qquad \Leftarrow \qquad \frac{\partial B_z}{\partial y} = \frac{\partial B_y}{\partial z} = -B_0\, b(y)\, k_{\mathrm{p}} \sin k_{\mathrm{p}} z$$
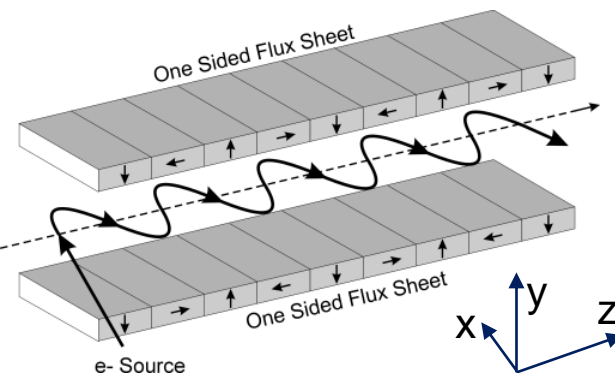
$$\text{and} \qquad B_y = -B_0\, b(y)(1 - \cos k_{\mathrm{p}} z)$$

$$\nabla \cdot \mathbf{B} = 0 \qquad \Leftarrow \qquad \frac{\partial B_z}{\partial z} = -B_0 \frac{\partial b(y)}{\partial y} \cos k_{\mathrm{p}} z$$

$$\mathbf{B} \neq \mathbf{B(x)}$$

$$\text{form} \quad \frac{\partial^2 B_z}{\partial y \partial z} \implies \frac{\partial^2 b(y)}{\partial^2 y} = k_{\mathrm{p}}^2\, b(y) \qquad \Leftarrow \qquad b(y) = a_1 \cosh k_{\mathrm{p}} y + a_2 \sinh k_{\mathrm{p}} y$$

One Sided Flux Sheet

One Sided Flux Sheet

e- Source

$$B_x = 0$$
$$B_y = B_0 \cosh k_{\mathrm{p}} y \cos k_{\mathrm{p}} z$$
$$B_z = -B_0 \sinh k_{\mathrm{p}} y \sin k_{\mathrm{p}} z$$

21

Assume x-axis is infinite in plan undulator

Spectrum features & calculation

Radiation from accelerator electron
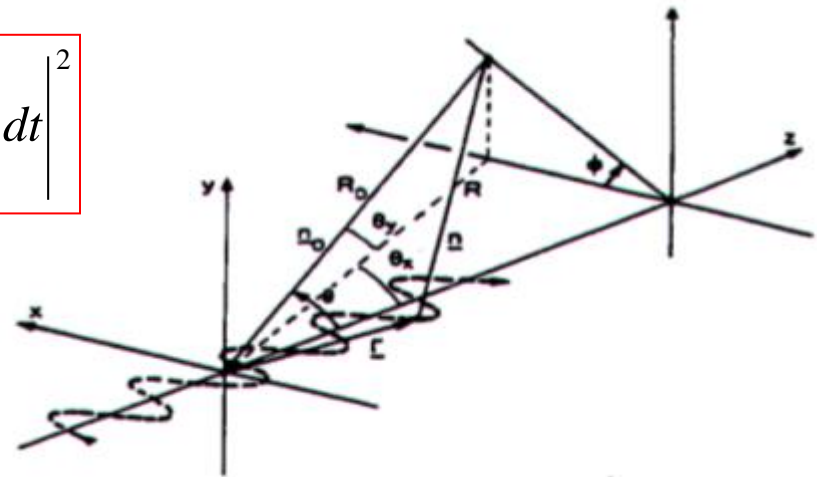
◆ Spectral/angular distribution

$$\frac{d^2 I}{d\omega d\Omega} = \frac{c}{4\pi^2} \left| \int_{-\infty}^{\infty} R E(t) e^{i\omega t} dt \right|^2 \qquad E(t) = \frac{e}{\sqrt{4\pi\varepsilon_o c}} \left[\frac{\hat{n} \wedge \{(\hat{n} - \beta) \wedge \dot{\beta}\}}{(1 - \hat{n} \cdot \beta)^3 R} \right]_{t_{ret.}}$$

where $\hat{n} = (\sin\theta\cos\phi, \sin\theta\sin\phi, \cos\theta)$ is the unit vector from the point of emission to the observer (see Figure). The observer and emission times are related by:

$t = t_{ret.} + R/c$ where R is the distance between the emission and observer points, and hence:

$$\frac{d^2 I}{d\omega d\Omega} = \frac{e^2}{(4\pi\varepsilon_o)4\pi^2 c} \left| \int_{-\infty}^{\infty} \frac{\hat{n} \wedge \{(\hat{n} - \beta) \wedge \beta\}}{(1 - \hat{n} \cdot \beta)^2} e^{i\omega(t - \hat{n} \cdot r/c)} dt \right|^2$$

$$\frac{d^2 I}{d\omega d\Omega} = \frac{e^2 \gamma^2 N^2}{(4\pi\varepsilon_o)c} L(N\Delta\omega / \omega_1(\theta)) F_n(K, \theta, \phi)$$

Geometry for the analysis of undulator radiation

General radiation formula

23

Radiation from bending & wiggler magnet

   In a wiggler, the deflection parameter K is large (typically $K{\geq}10$) and photon radiation from different poles of the electron trajectory is enhanced incoherently. The angular density of flux is then given by 2N (N is the number of magnet periods) times the formula for bending magnets. *The angular distribution of radiation emitted by electrons that are moving through a bending magnet, following a circular trajectory in a horizontal plane is,*

$$\frac{d^2\bar{B}(w)}{d\theta d\phi} = \frac{3\alpha\gamma^2}{4\pi^2}\frac{I}{e}\frac{\Delta w}{w}\left(\frac{\varepsilon}{\varepsilon_c}\right)^2\left(1+\gamma^2\phi^2\right)^2\left[\underset{\sigma\text{-mode}}{K_{2/3}^2(\xi)}+\frac{\gamma^2\phi^2}{1+\gamma^2\phi^2}\underset{\pi\text{- mode}}{K_{1/3}^2(\xi)}\right]$$

*Where ε and ε_c are the photon energy and the photon critical energy, respectively; θ and ϕ are the observation angles in the horizontal and vertical directions, respectively*; α is the fine-structure constant; I is the beam current; e is the electron charge; the subscripted K's are modified Bessel functions of the second kind, and *ξ is defined as*

$$\varepsilon_c(\text{keV}) = 0.665\text{E}^2(\text{GeV})\text{B(T)}$$

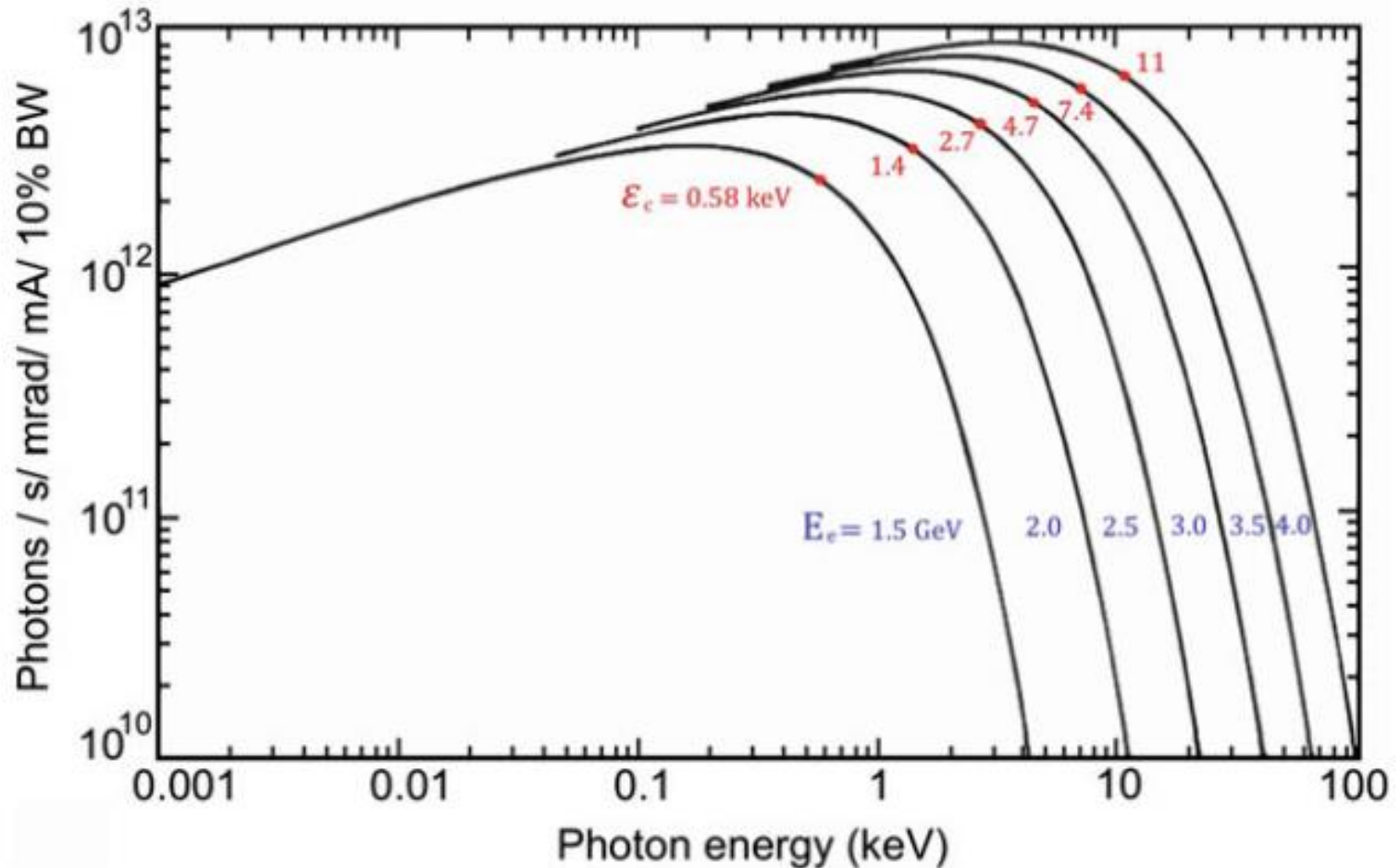$$\xi \equiv \left(\varepsilon/2\varepsilon_c\right)\left(1+\gamma^2\phi^2\right)^{3/2}$$

$$\varepsilon_c(\theta) = \varepsilon_c(0)\sqrt{1-\left(\gamma\theta/K\right)^2}$$

Radiation distribution on π-σ mode

π- mode

σ-mode
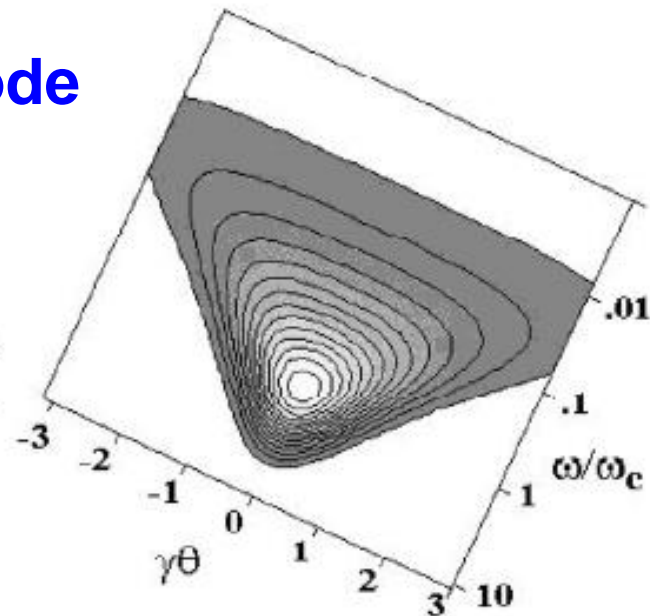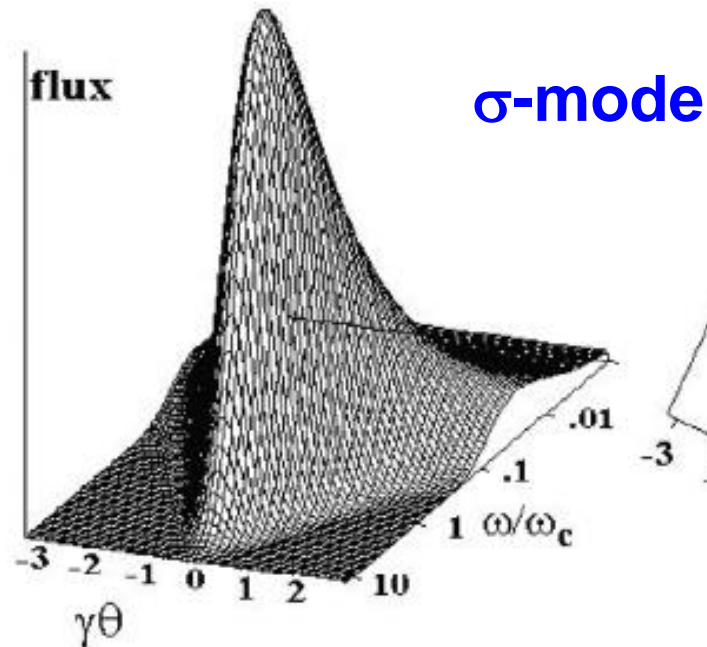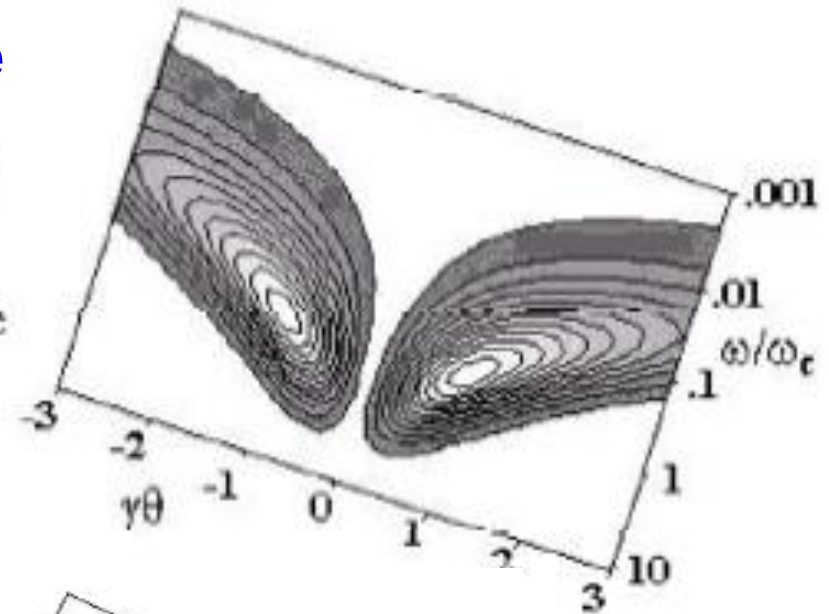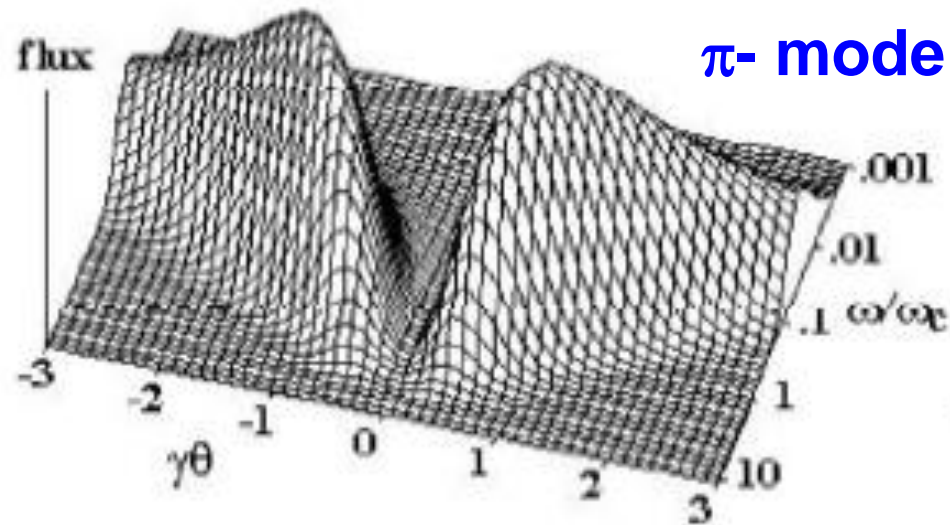
$$\varepsilon_c \, (\text{keV}) = 0.665 E^2(\text{GeV}) B(\text{T})$$

$$\varepsilon_c(\theta) = \varepsilon_c(0)\sqrt{1-\left(\gamma\theta \, / \, K\right)^2}$$

Flux Density
$$\frac{d^2 F(w)}{d\theta d\phi}[p/s/mrad^2] = 1.327 \times 10^{16} \frac{\Delta w}{w} E^2 [GeV] I[A] H_2(y)$$

Flux Density distribution integrated over ϕ is given by

$$\frac{d\ F(w)}{d\theta}[p/s/mrad\ ] = 2.457 \times 10^{16} \frac{\Delta w}{w} E\ [GeV] I[A] G_1(y)$$

At $\phi = 0$
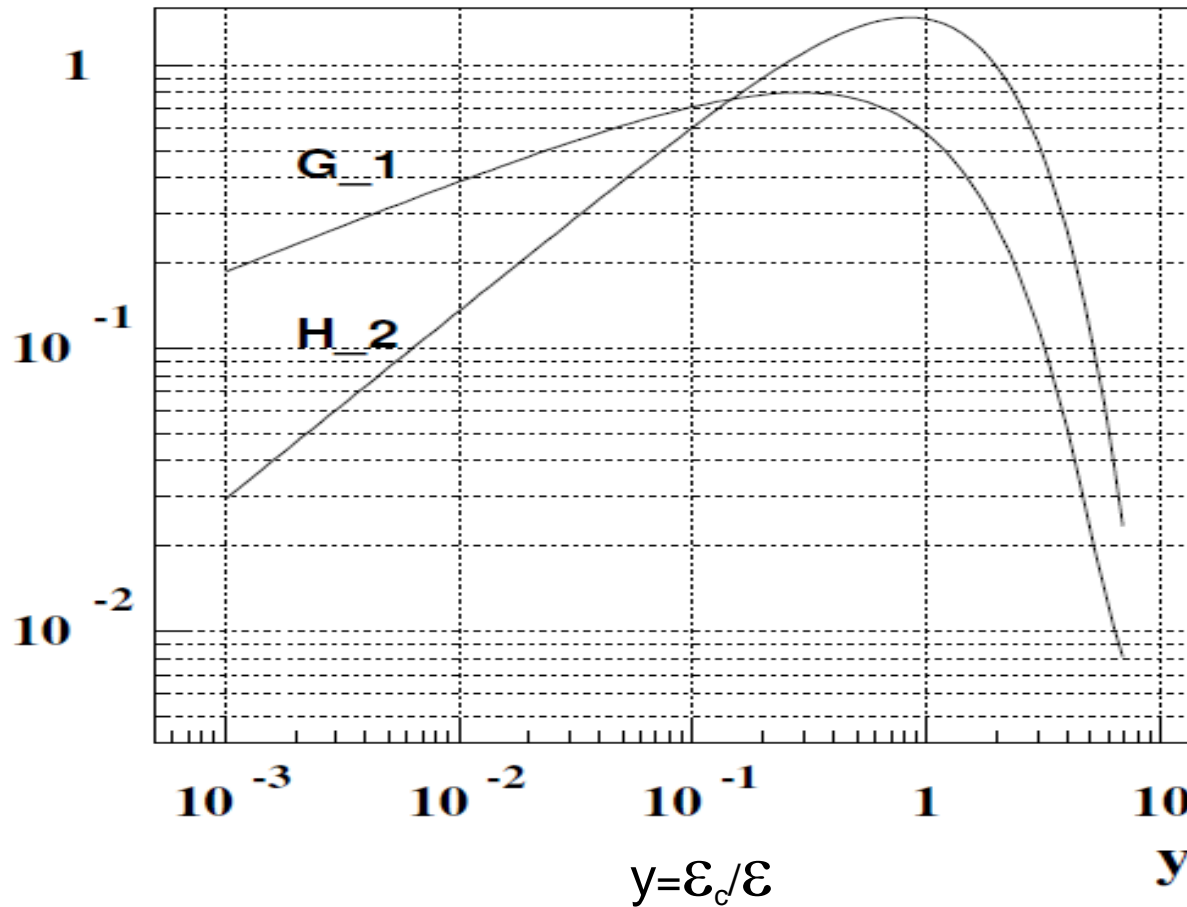$$\frac{d^2 F(w)}{d\theta d\phi} = \frac{d\ F(w)}{d\theta} \cdot \frac{1}{\sigma_\phi \sqrt{2\pi}}$$

Therefore, the total flux F(w) of bending radiation is integrated over θ . However, for the wiggler radiation, the total flux F(w) will be multiplied by a factor of 2N (N is the period number).

$$\frac{d\ F(w)}{d\theta}[p/s/mrad] = 2.457 \times 10^{16} \frac{\Delta w}{w} E\ 2N[GeV] I[A] G_1(y)$$

Finally, the power density or total power is flux density or total flux multiply by photon energy, respectively.

27

$$y = \varepsilon_c / \varepsilon$$

$$\frac{d^2 F(w)}{d\theta d\phi}[p/s/mrad^2/0.1\%BW] = 1.327 \times 10^{13} E^2 [GeV] I[A] H_2(y)$$

$$\frac{d F(w)}{d\theta}[p/s/mrad/0.1\%BW] = 2.457 \times 10^{13} E[GeV] I[A] G_1(y)$$

28

Electron motion in the Insertion Devices

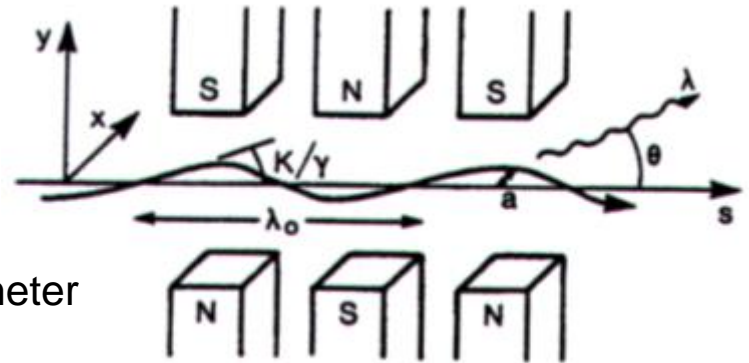$B_y = B_0 \sin(kz)$, where $k = 2\pi / \lambda_0$ and λ_0 is the insertion device period length.

$$\ddot{x} = \frac{e}{\gamma m}\left(-\dot{z}B_y\right) \qquad \ddot{z} = \frac{e}{\gamma m}\left(\dot{x}B_y\right)$$

$$\dot{x} = \frac{eB_o}{\gamma m}\frac{\cos(kz)}{k} \qquad \beta_x = \dot{x}/c = \frac{K}{\gamma}\cos(kz)$$

where the dimensionless undulator or deflection parameter is defined as follows:

$$\boxed{K = \frac{eB_o\lambda_o}{2\pi mc} = 0.934 B_o[T]\lambda_o[cm]}$$

$$\beta_z \cong \beta\left(1 - \frac{K^2}{4\gamma^2} - \frac{K^2}{4\gamma^2}\cos 2kz\right)$$

$$\beta_x^2 + \beta_z^2 = \beta^2 \quad (= \text{constant})$$

First integral field ∫Bds=0 (x'=0) & Second integral field ∫(∫ Bds')ds=0 (x=0)

The average velocity along the z-axis is thus:
$$\overline{\beta} \cong \beta\left(1 - \frac{K^2}{4\gamma^2}\right) \cong 1 - \frac{1}{2\gamma^2} - \frac{K^2}{4\gamma^2}$$

We will only consider cases in which $K/\gamma \ll 1$ and so we can write to a good approximation that

$z = \overline{\beta}ct$ and $kz = \Omega t$ where $\Omega = 2\pi\overline{\beta}c / \lambda_o$. We have electron angle then:

$$\dot{x} = \frac{K}{\gamma}c\cos(\Omega t) \quad \text{which can be integrated directly to give e-trajectory:} \quad x = \frac{K}{\gamma}\frac{c}{\Omega}\sin(\Omega t)$$

$$x' = \frac{K}{\gamma}\cos(\Omega t), \quad z = \overline{\beta}ct - \frac{K^2}{4\gamma^2}\frac{c}{2\Omega}\sin(2\Omega t), \quad \dot{z} = \overline{\beta}c - \frac{K^2}{4\gamma^2}c\cos(2\Omega t), \quad \boxed{x = \frac{K}{\gamma}\frac{\lambda_0}{2\pi},} \quad \boxed{x' = \frac{K}{\gamma}}$$

Photon Interference in undulator

In the time it takes the electron to move through one period length from point A to an equivalent point B ($\lambda_o / \bar{\beta} c$) the wavefront from A has advanced by a distance $\lambda_o / \bar{\beta}$ and hence is ahead of the radiation emitted at point B by a distance *d* where:

$$d = \frac{\lambda_o}{\bar{\beta}} - \lambda_o \cos \theta$$

and where *θ* is the angle of emission with respect to the electron beam axis. When this distance is equal to an integral number, *n*, of radiation wavelength there is constructive interference of the radiation from successive poles:

$$\frac{\lambda_o}{\bar{\beta}} - \lambda_o \cos \theta = n\lambda$$

Inserting the expression for the average electron velocity:

$$\frac{1}{\bar{\beta}} \cong 1 + \frac{1}{2\gamma^2} + \frac{K^2}{4\gamma^2}$$

results in the following interference condition:

$K >> 1$ wiggler, $K \approx 1$ undulator,

$$\varepsilon \left[keV \right] = 0.95 n \frac{E^2 \left[GeV \right]}{\lambda_o \left(1 + \frac{K^2}{2} + \gamma^2 \left(\theta^2 + \phi^2 \right) \right)}$$

$$\varepsilon \left[eV \right] = \frac{1.2398}{\lambda_p (\mu m)}$$

$$\lambda (A) = \frac{\lambda_0 (mm)}{2n\gamma^2} \left(1 + \frac{K^2}{2} + \gamma^2 \left(\theta^2 + \phi^2 \right) \right) = 1305.6 \frac{\lambda_p (m)(1 + \frac{K^2}{2} + \gamma^2 \left(\theta^2 + \phi^2 \right))}{nE(GeV)^2}$$
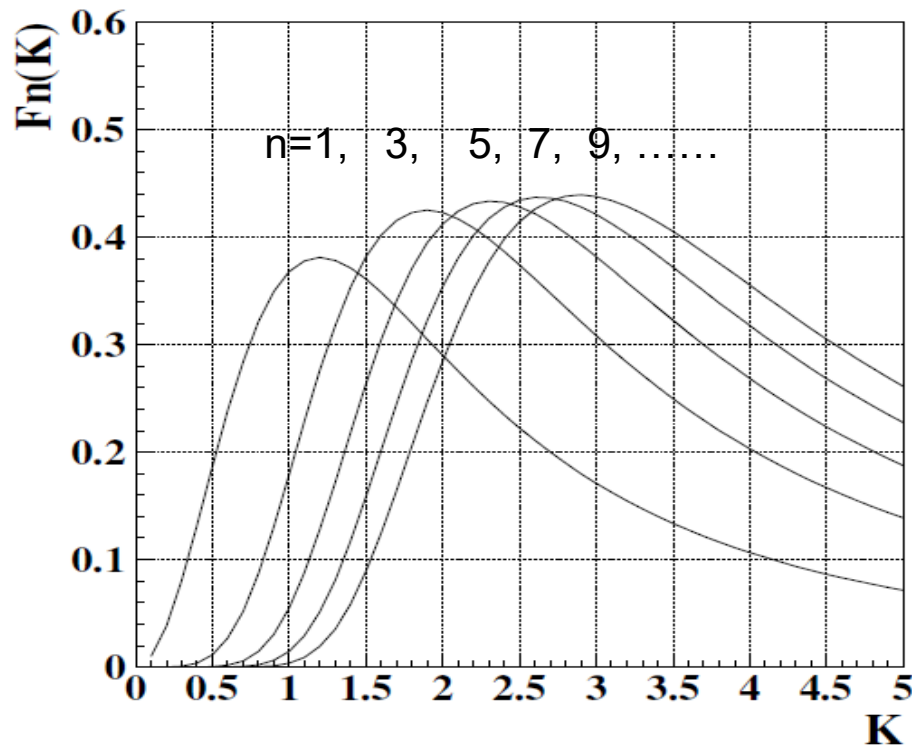
30

F function of Angular flux density in the horizontal (left) and vertical (right) planes for the case $K = 1$. $\boxed{K = 0.934 B_o [T] \lambda_o [cm]}$

$$F_n(K) = \frac{n^2 K^2}{\left(1 + K^2/2\right)^2} \left[J_{\frac{n+1}{2}}(Z) - J_{\frac{n-1}{2}}(Z) \right]^2 \qquad Z = \frac{nK^2}{4\left(1 + K^2/2\right)}$$

On-axis ($\theta = \phi = 0$)

Angular flux density from undulator-2

n=1, 3, 5, 7, 9, ……

On-axis angular flux density function

in practical units of photons/s/mrad²/0.1% bandwidth:

If k ≤2 only n=1,3,5,7,9,11,13,15;
  k ≤1 only n=1,3,5,7; k ≤0.5 only n=1,3
  k ≤0.25 only n=1

If n=1 -> K_{min}=0.15; n=3 -> K_{min}=0.5;
  n=5 -> K_{min}=0.75; n=7 -> K_{min}= 1;
  n=9 -> K_{min}=1.2 ; n=11 -> K_{min}=1.4

$$\varepsilon\,[keV] = 0.95n \frac{E^2\,[GeV]}{\lambda_o\left(1+\frac{K^2}{2}+\gamma^2\left(\theta^2+\phi^2\right)\right)}$$

$$K = \frac{eB_o\lambda_o}{2\pi mc} = 0.934 B_o\,[T]\lambda_o\,[cm]$$

$$\overline{\beta} = \frac{d^2\dot{n}}{d\omega/\omega\cdot d\Omega}\bigg|_{\theta=0} \quad [p/s/rad^2/0.1\%\,BW] = 1.744\cdot10^{20}N^2E^2\,[GeV]F_n(K)I_b(A)$$

$$\overline{\beta} = \frac{d^2\dot{n}}{d\Omega}\bigg|_{\theta=0} \quad [p/s/rad^2] = 1.744\cdot10^{23}N^2E^2\,[GeV]F_n(K)I_b(A)$$

◆ Total flux

We obtain the total flux in the central cone in practical units of flux is photons/s/0.1% bandwidth:

$$B = \bar{B}d\Omega = \frac{d\dot{n}}{d\omega/\omega} = 1.431 \cdot 10^{14} N Q_n(K) f\left(N\Delta\omega / \omega_1(0)\right) I_b$$

where $Q_n(K) = \left(1 + K^2/2\right) F_n(K)/n$. The flux function $Q_n(K)$ and the detuning function $f\left(N\Delta\omega / \omega_1(0)\right)$. It can be seen that for zero detuning (i.e. $\omega = \omega_n(0)$) the flux is very close to half of the usually quoted result. Nearly twice as much flux can be obtained however by a small detuning to lower frequency by approximately
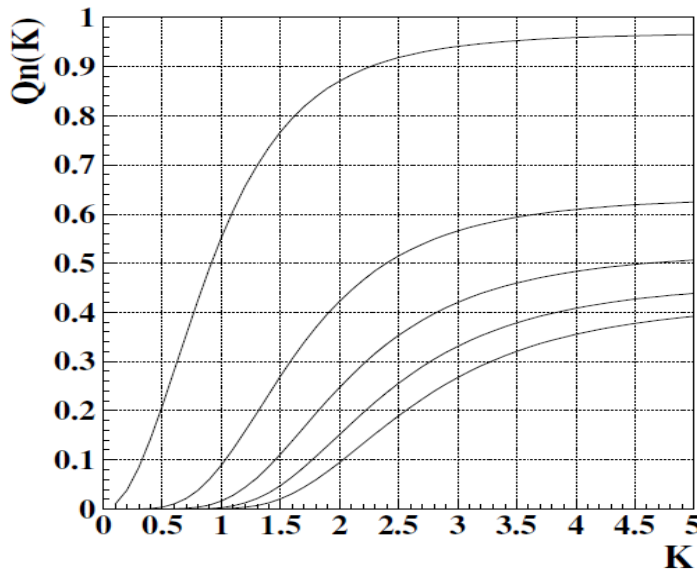
$Q_n(k)$: Undulator flux function
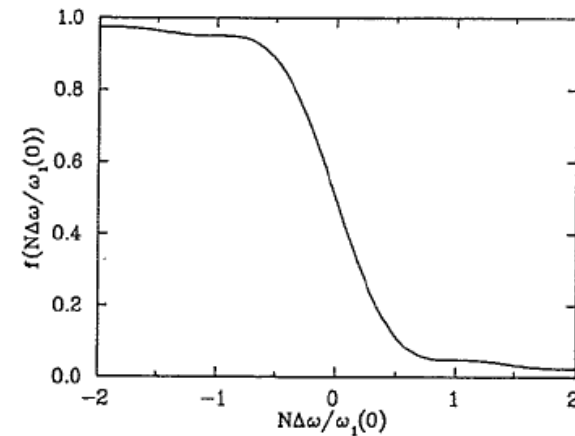
Undulator flux function as function of detuning

◆ Power and power density

$$\frac{d^2\dot{n}}{d\omega/\omega \cdot d\Omega} \times E_P = \frac{dP}{d\Omega}\left[W/mrad^2\right] = 10.84 E^4[GeV] B_o N I_b G(K) f_K(\theta_x, \theta_y)$$

where $G(K) = \dfrac{K\left(K^6 + \frac{24}{7}K^4 + 4K^2 + \frac{16}{7}\right)}{\left(1+K^2\right)^{7/2}}$ and

$$f_K(\theta_x,\theta_y) = \frac{16K}{7\pi G(K)} \int_{-\pi}^{\pi} \sin^2\alpha\left[\frac{1}{D^3} - \frac{4(\gamma\theta_x - K\cos\alpha)^2}{D^5}\right]d\alpha$$, as obtained by Kim.

$f_K(\theta_x, \psi_y)$
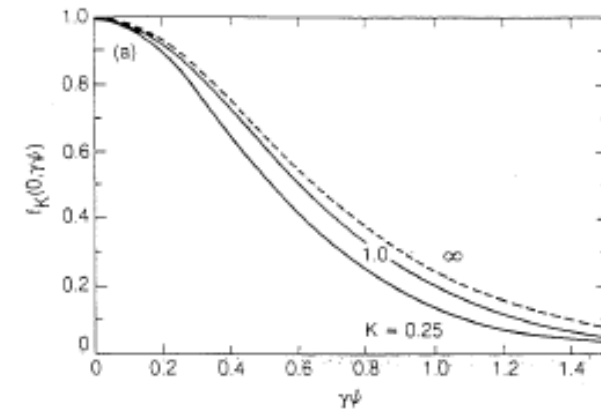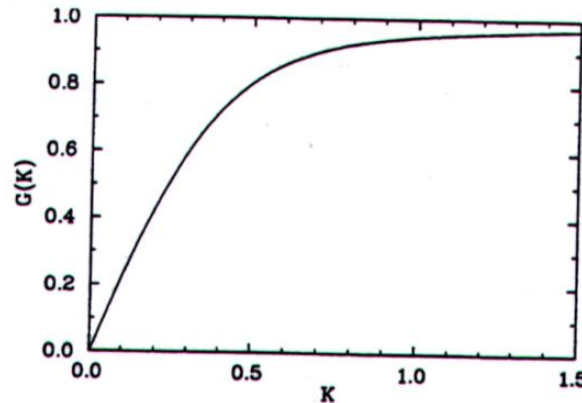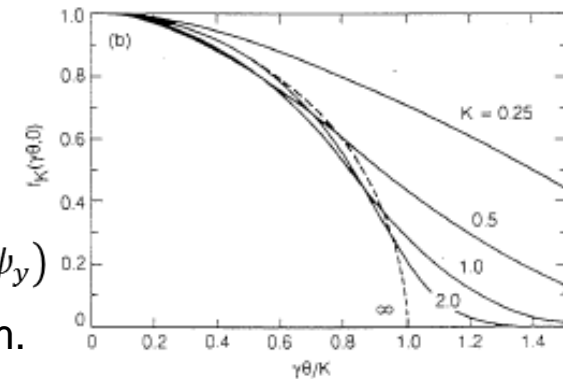
- Total power on ID

$$P_{tot}[kW] = 0.633 \cdot E^2[GeV] B_o^2 L I_b$$

- Total power on Bending magnet

$$P_{tot}[kW] = 0.633 \cdot E^2[GeV] 2 B_o^2 L I_b$$

Function of the calculation of the power density
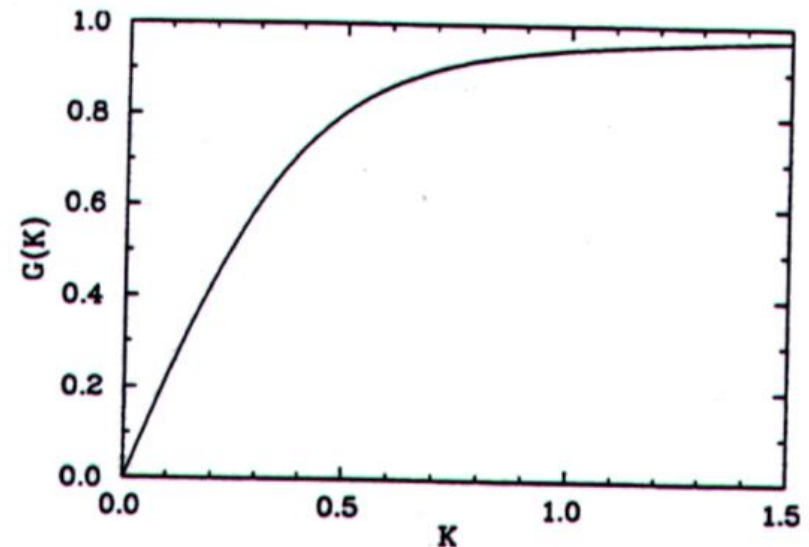
The function $G(K)$

$$P_{tot}[kW] = 0.633 \cdot E^2[GeV] B_o^2 L I_b$$

$$P\left[W/mrad^2\right] = 10.84 \cdot E^4[GeV] B_o[T] NI[A] G(k) f_k \ (\gamma\theta, \gamma\Psi)$$

35

Brightness

We will obtain the brightness in practical units is photon/s/mm²/mrad²/0.1% bandwidth. Photon flux unit is photon/s/0.1% bandwidth.

$$Brilliance(\beta) = \frac{photon \quad flux(B)}{4\pi^2 \sigma_x \sigma_y \sigma'_x \sigma'_y \left. \sigma_{BW} \right/ E}$$

$$\frac{\sigma_{BW}}{E} \approx \sqrt{\left(\frac{0.85}{nN_w}\right)^2 + \left(\frac{\sigma_E}{E}\right)^2}$$

$$\sigma_x = \sqrt{\varepsilon_x \beta_x + \eta^2 (\sigma_E/E)^2 + \sigma_{ph}^2}$$

$$\sigma'_x = \sqrt{\varepsilon_x \gamma_x + \eta'^2 (\sigma_E/E)^2 + \sigma'^2_{ph}}$$

$$\sigma_y = \sqrt{\varepsilon_y \beta_y + \sigma_{ph}^2}$$

$$\sigma'_y = \sqrt{\varepsilon_y \gamma_y + \sigma'^2_{ph}}$$

$$\gamma_{x,y}(s) = (1 + \alpha_{x,y}(s)^2)/\beta_{x,y}(s), \quad \alpha_{x,y}(s) = -\frac{1}{2}\frac{d\beta_{x,y}(s)}{ds}, \quad \beta_{x,y}(s) = \beta_{x,y}(0) + \frac{s^2}{\beta_{x,y}(0)}$$

The diffraction-limited source size (rms) $\sigma_{ph}\sigma'_{ph} = \frac{\lambda}{4\pi}$

corresponding to the angular divergence of ID $\sigma'_{ph} = \sqrt{\lambda_n/L} = \frac{1}{\gamma}\sqrt{\frac{1 + \left. k^2 \right/ 2}{2N \cdot n}}$

λ is the photon wavelength and λ_u is the undulator periodic length.

corresponding to the angular divergence of bending magnet $\sigma'_{ph}(mr) = 0.48\frac{C(y)}{E(GeV)}$

36

Example of the characteristics of ID spectrum
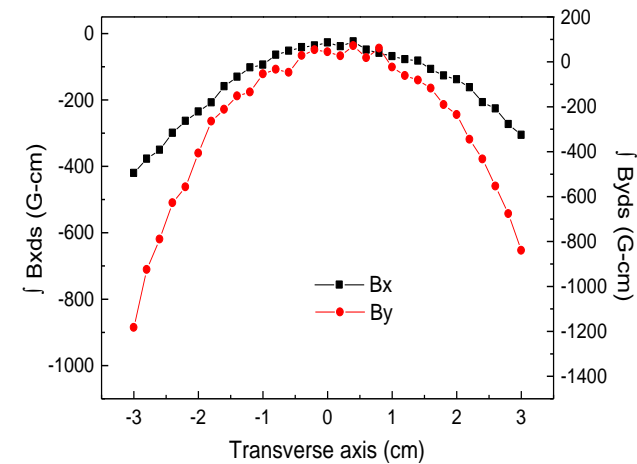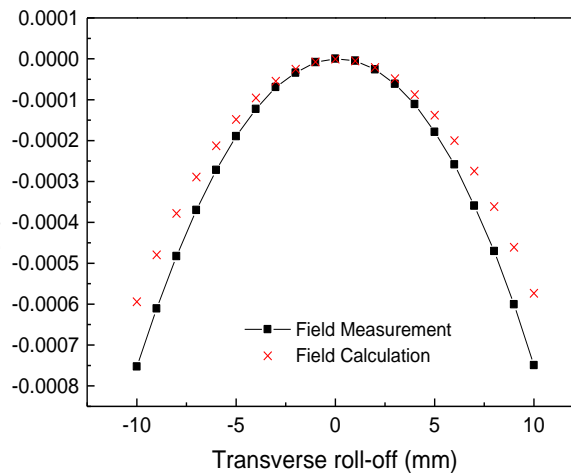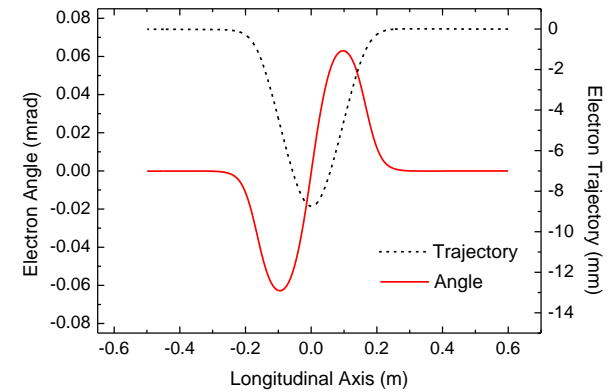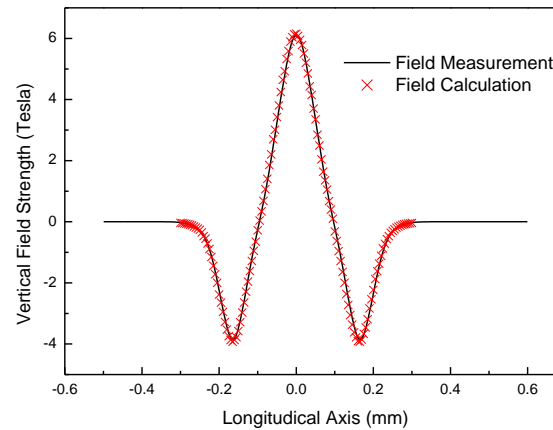
Features of elliptically polarized undulator

EPU5.6 (Bx=By=0.444 T)

Phot/s/0.1%bw/mr^2

Photon Energy (keV)
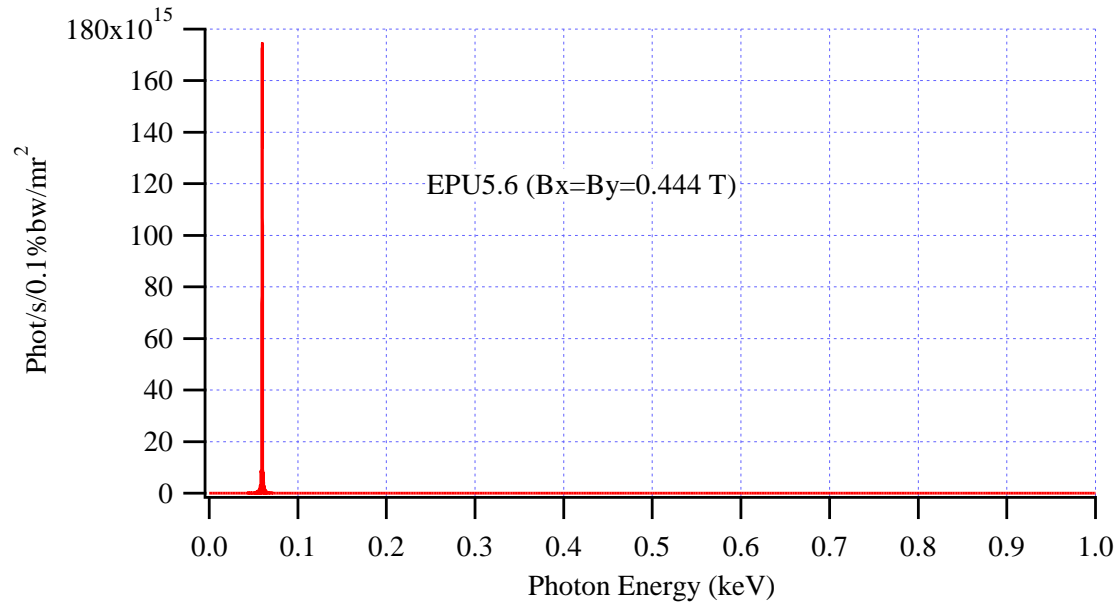
Circular polarization n=1,
 higher harmonic spectrum is zero

EPU5.6 (Bx=0.24 T, By=0.6 T)

Phot/s/0.1%bw/mr^2

Photon Energy (keV)
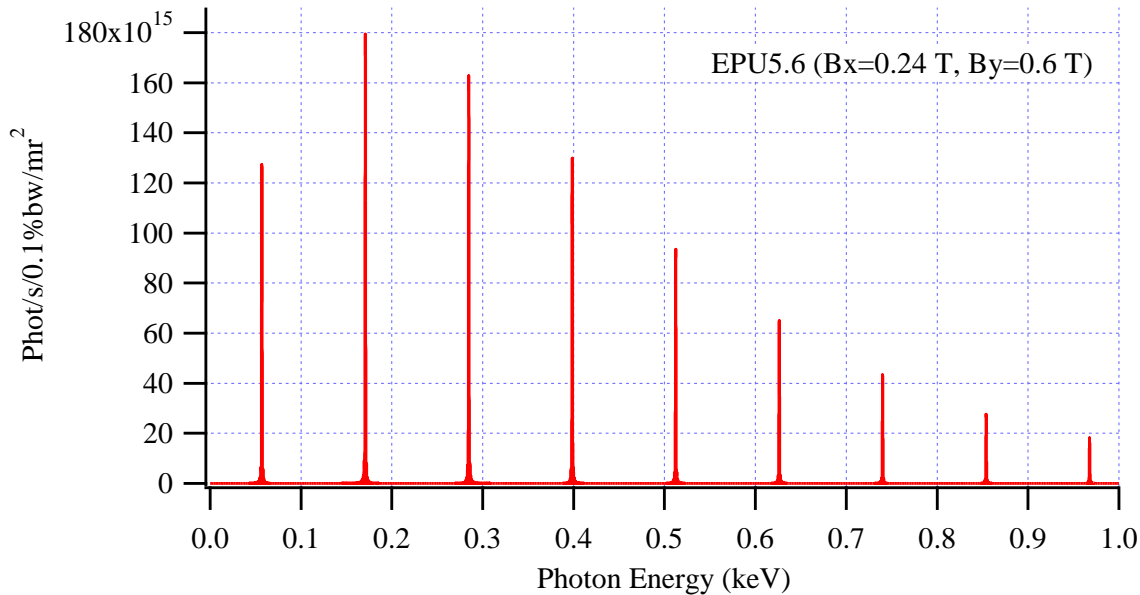
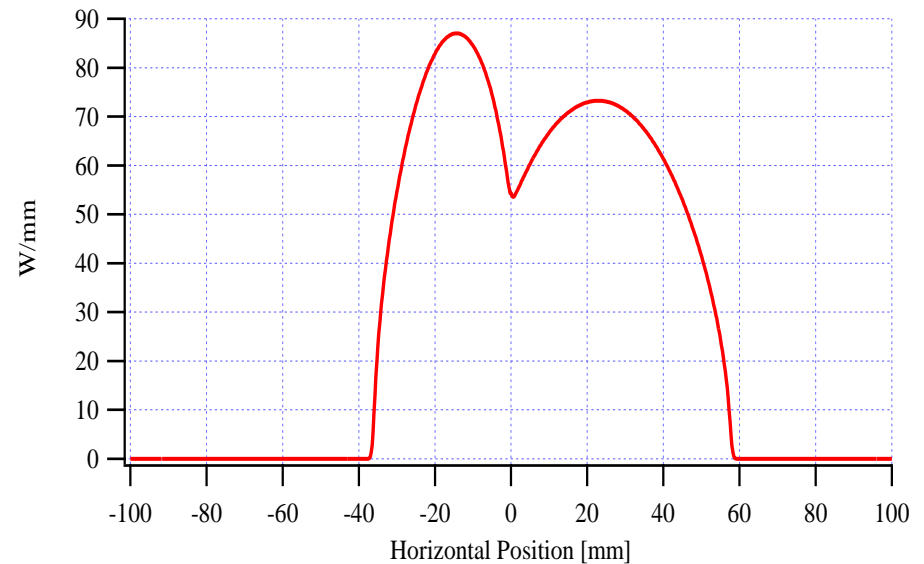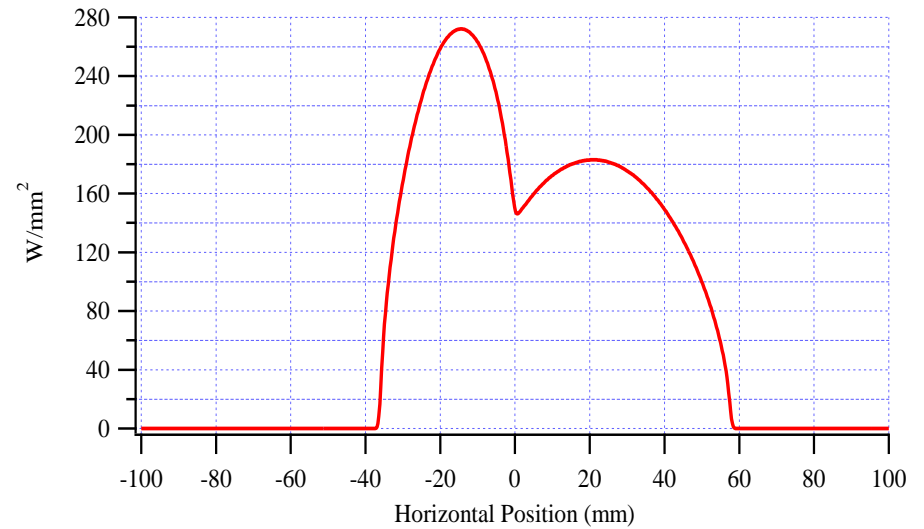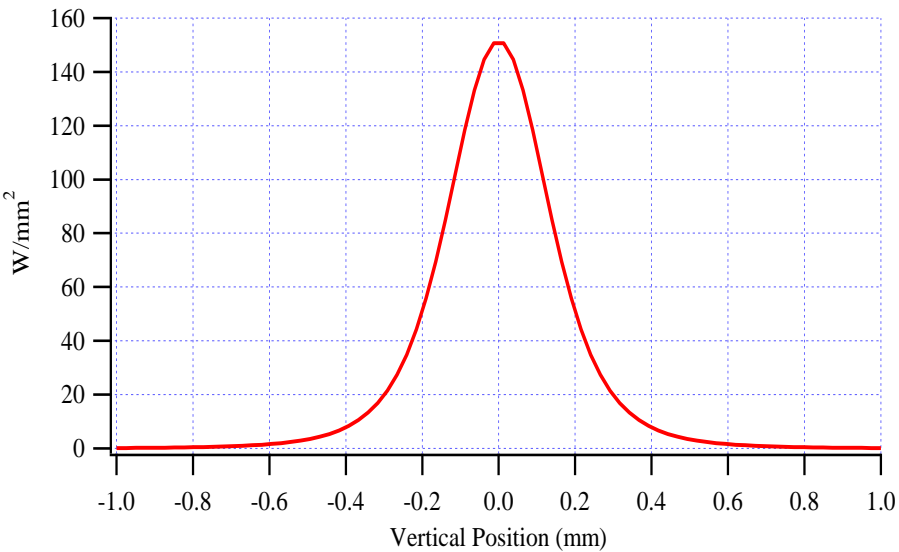Elliptical polarization for fundamental
and higher harmonic spectrum

38

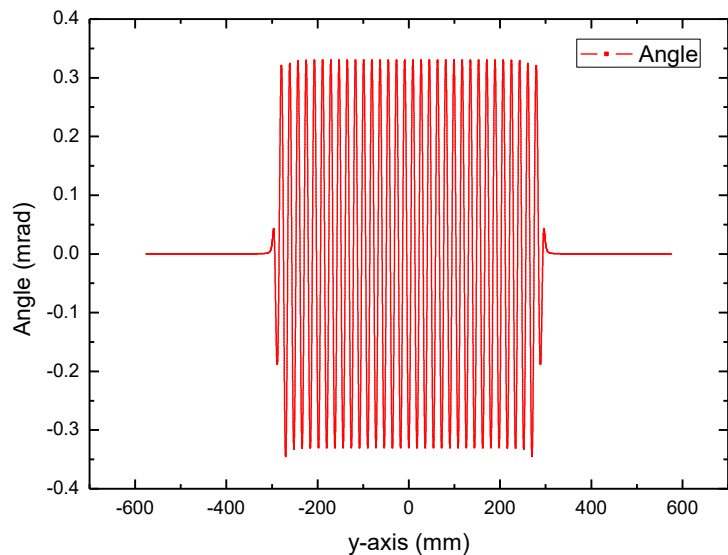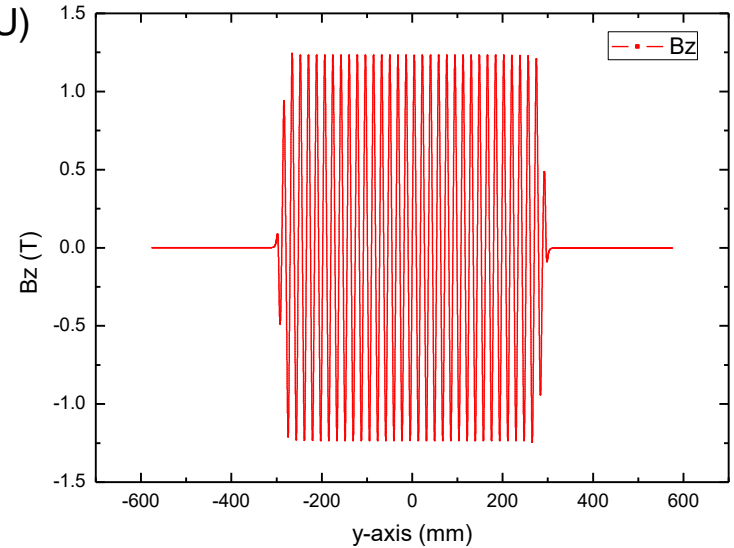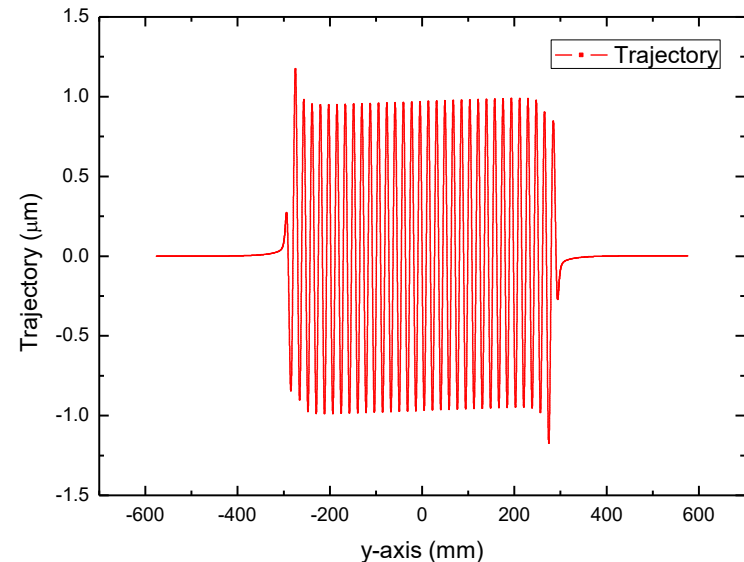# Power density calculation (total 5.96 kW)
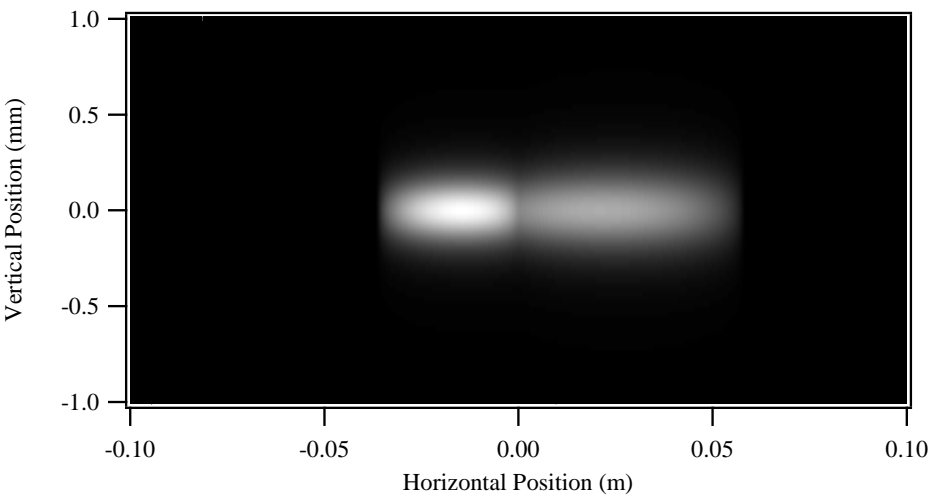
Away from source 0.7 m

Field, first & second field integral of CU22
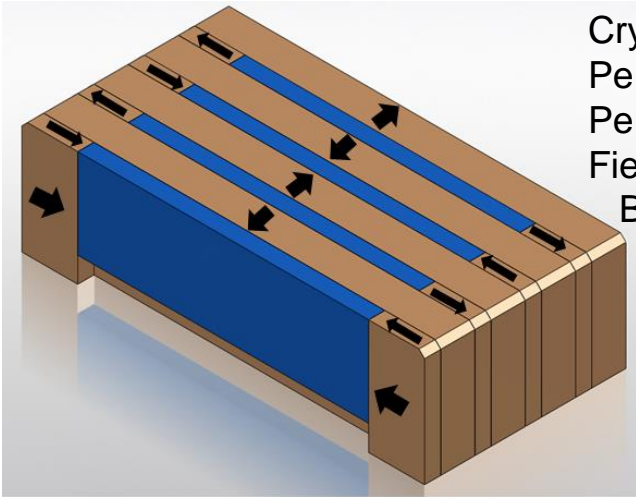
Cryogenic undulator (CU)
Period length: 18 mm,
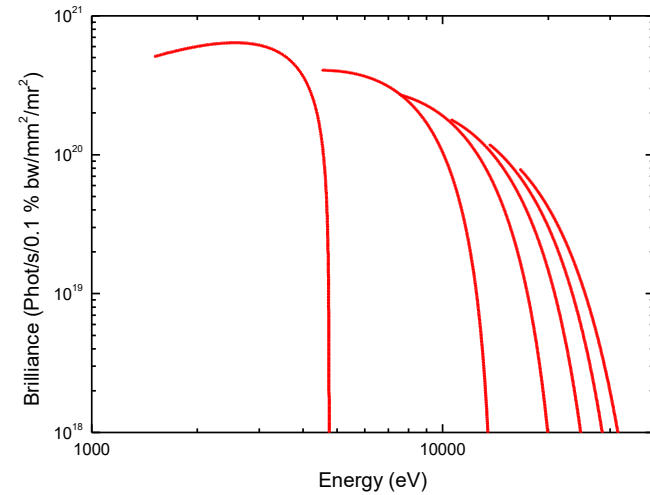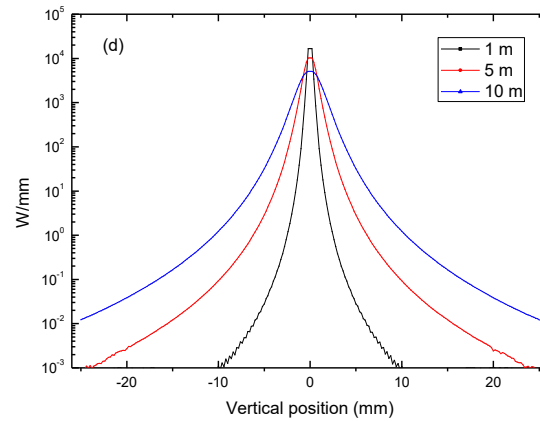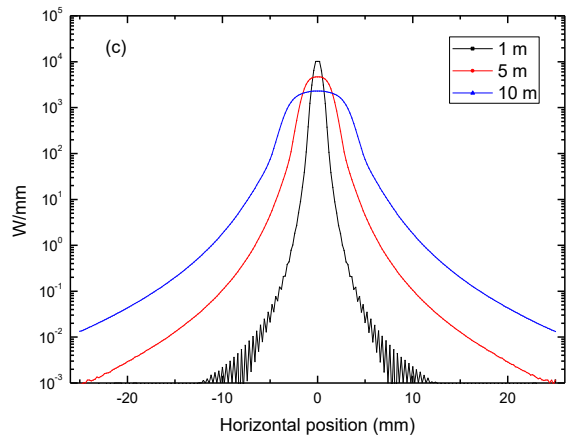Period number: 170,
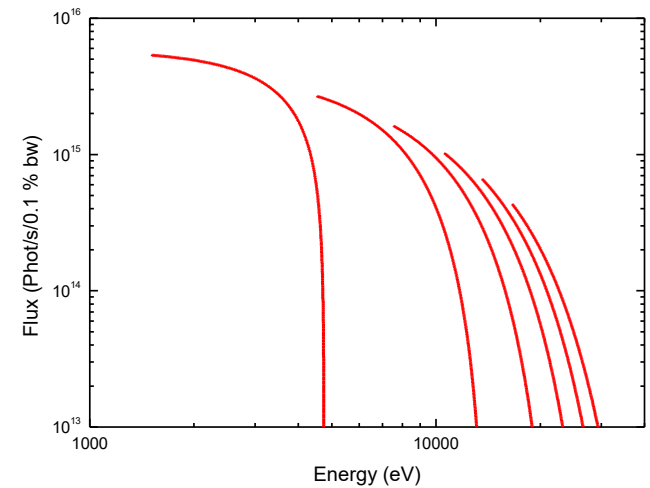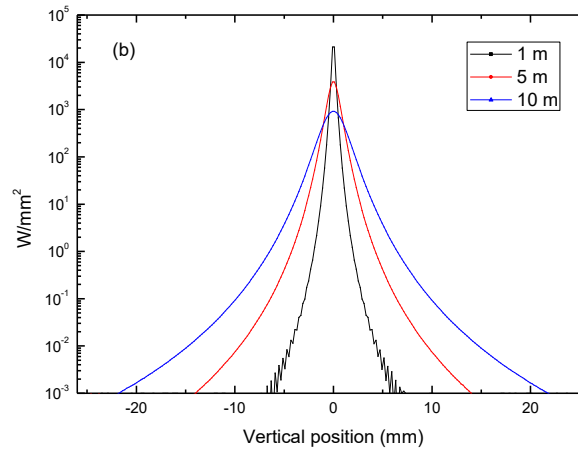Field strength: 1.23 T,
  B_r=1.5 T @ 135K

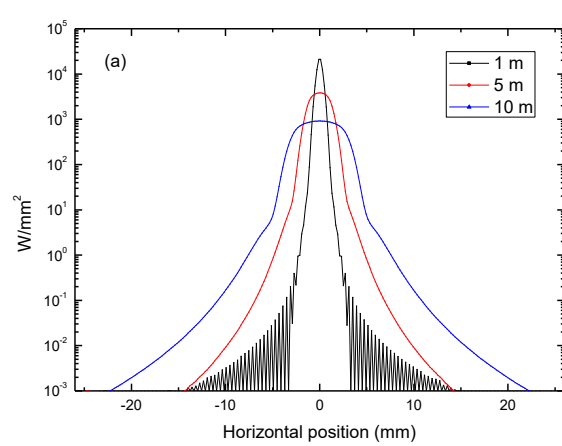$$x' = \frac{K}{\gamma}\cos(\Omega t),$$

$$x = \frac{K}{\gamma}\frac{\lambda_u}{2\pi}\sin(\Omega t)$$
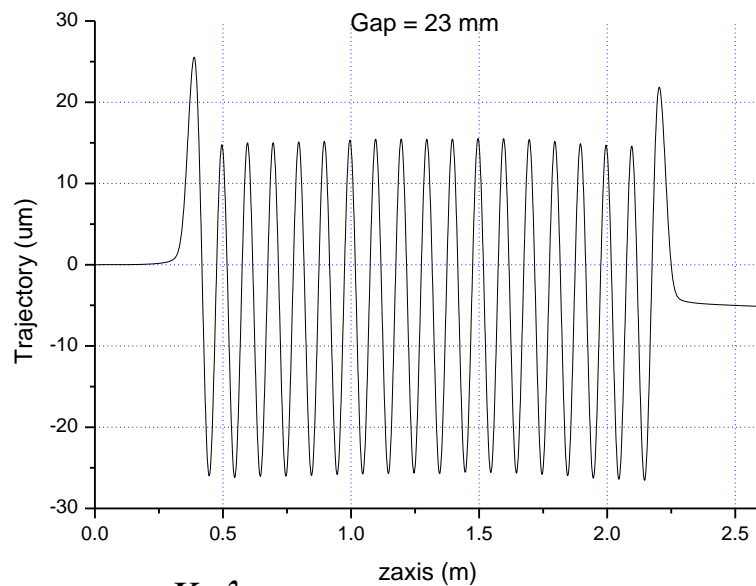
41

Spectra and power distribution of CU22

power distribution

spectrum

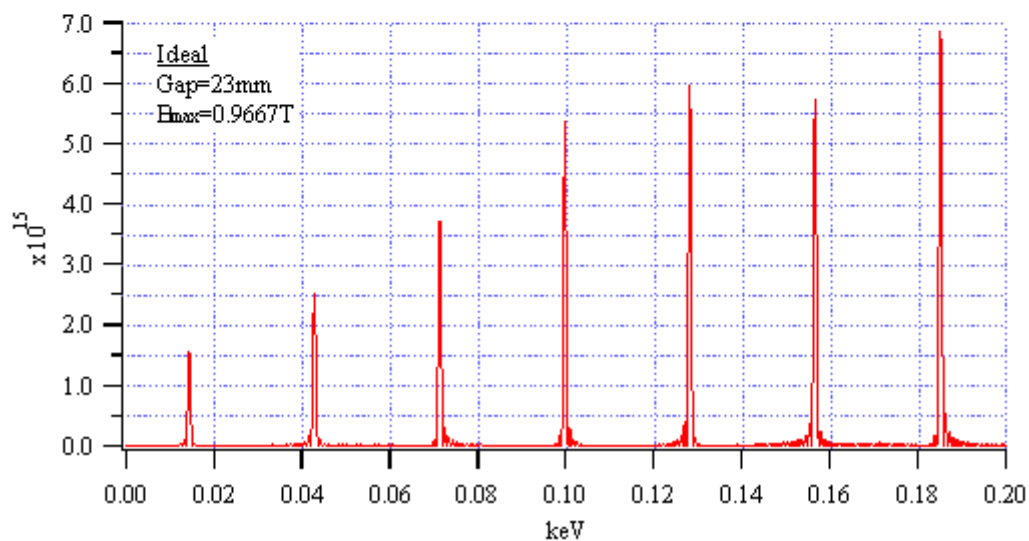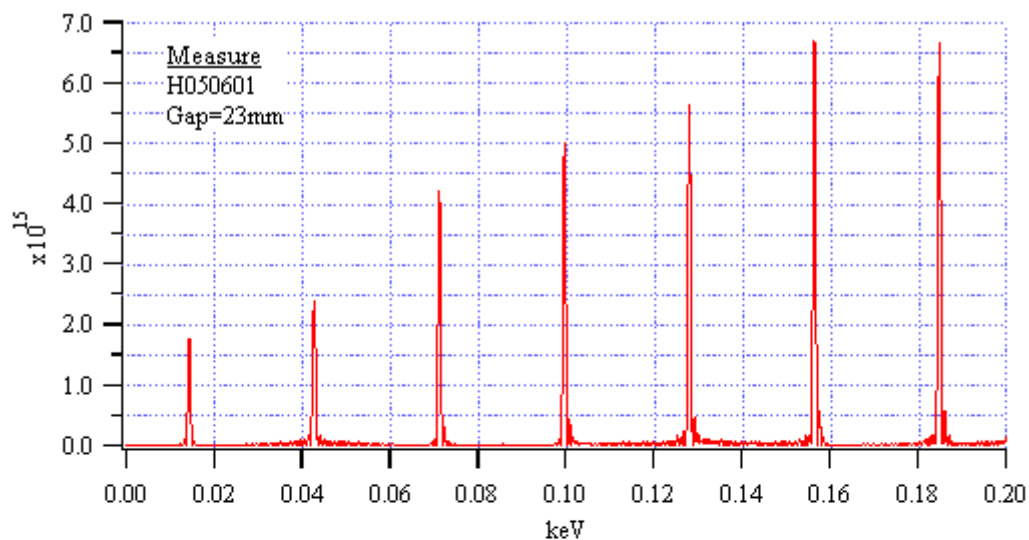# U100 field distribution- example

$$B_y = B_0 \sin(kz),$$
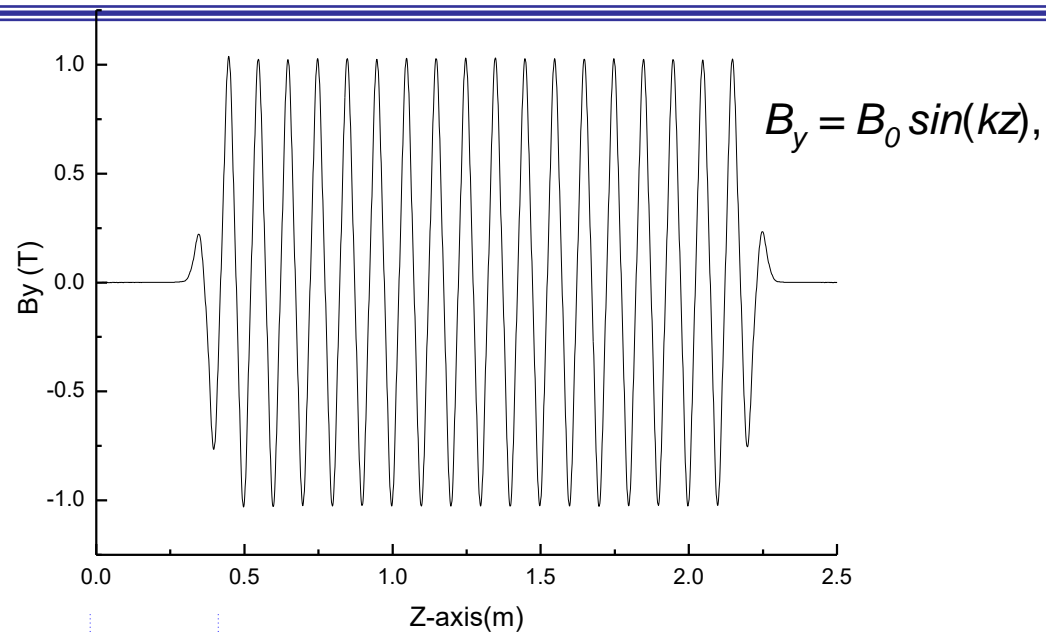
$$x = \frac{K}{\gamma} \frac{\lambda_u}{2\pi} \sin(\Omega t)$$
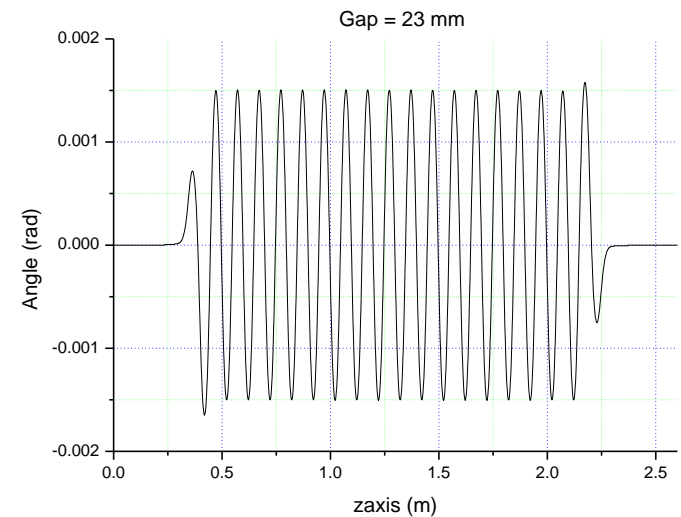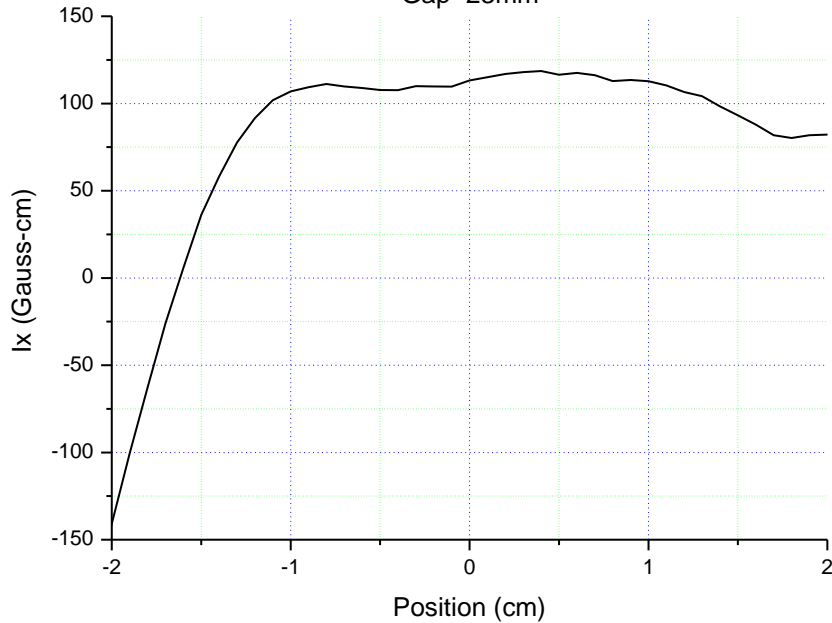
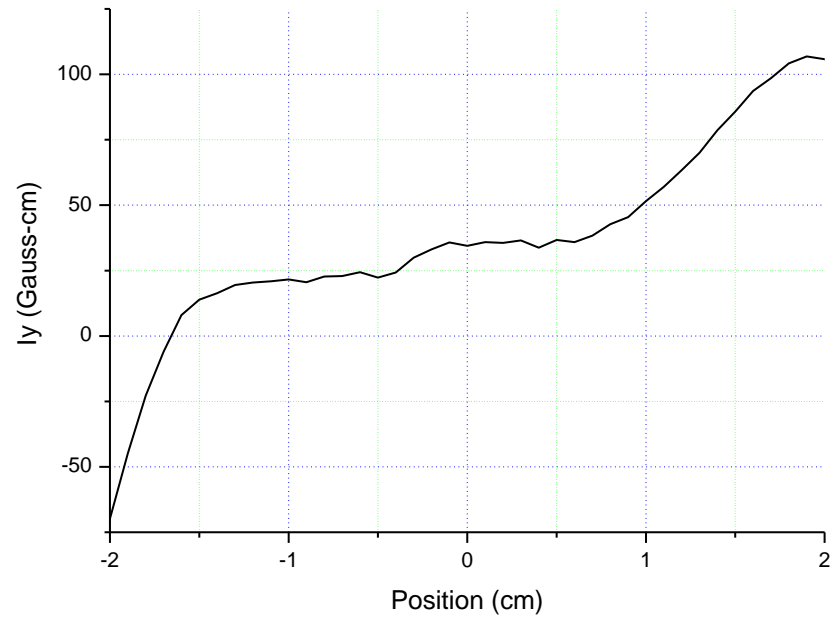$$x' = \frac{K}{\gamma} \cos(\Omega t),$$

U100 spectrum- example

U100 Integral multipole- example

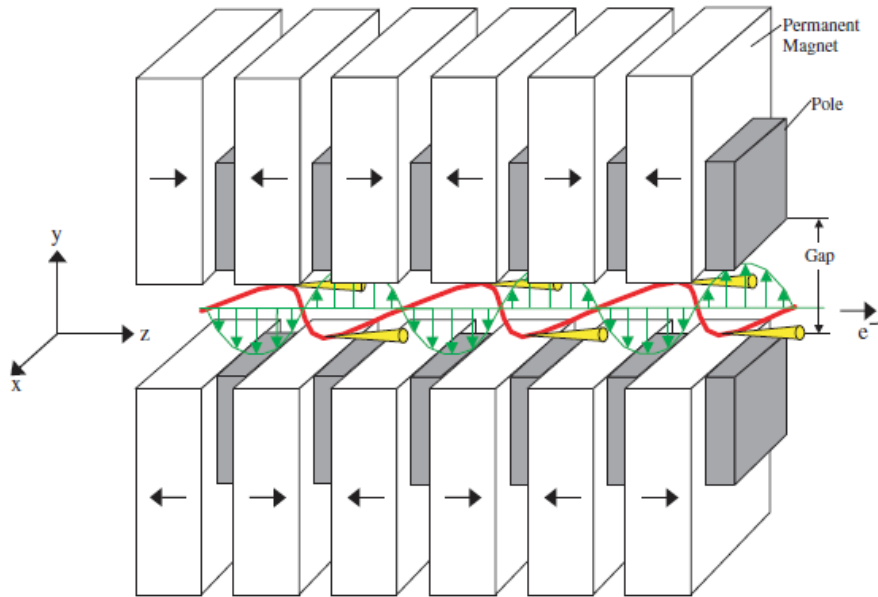# How to design and shimming ID

Spectra calculation code

Advantages	Disadvantages
SRW (ESFR):	
* User friendly package;	* Training course needed for familiarization;
* Associated with slit for beam line design;	* Documentation is not clear;
* Easy to do data process and data analysis;	* Large computer needed;
* Calculation spectrum & power distribution;	* Program is not yet completed;
* For simple field calculation;	* Some parameters are not included;
* Fast calculation for FFT analysis spectrum	* Can down load from ESRF website
* Run in PC	
Spectra (SPing8):	
* User friendly package	* Training course needed for familiarization;
* Calculation spectrum & power distribution	* Large use of memory;
* Easy to put parameters and data process	* Documentation is not clear;
* Taking into account different bata function	* Program is not yet completed;
* Fast calculation	* Can down load from SPring8 website
* Run in PC	

Magnet computation codes for magnet design

Advantages	Disadvantages
TOSCA:	
* Full three dimensional package;	* Training course needed for familiarization;
* Accurate prediction of distribution and strength in 3D;	* Expensive to purchase;
* Extensive pre/post-processing;	* Large computer needed.
* Multipole function and Fast calculation	* Large use of memory.
* For static & DC & AC field calculation	* Cpu time is hours for non-linear 3D problem.
* Run in PC or workstation	* It can be run combined field
RADIA:	
* Full three dimensional package	* Larger computer needed
* Accurate prediction of distribution and strength in 3D	* Large use of memory
	* Be careful to make segmentation
* With quick-time to view and rotate 3D structure	* Only DC field calculation
* Easy to build model with mathematic	
* Easy to perform data analysis and data polt	* Can down load from ESRF website
* Run in PC	

Magnet circuit type

Hybrid structure

Pure structure

49
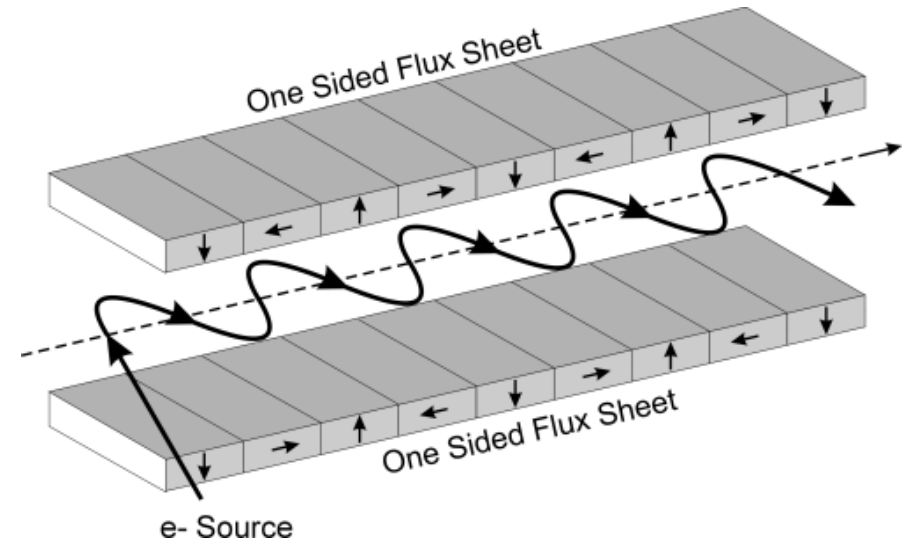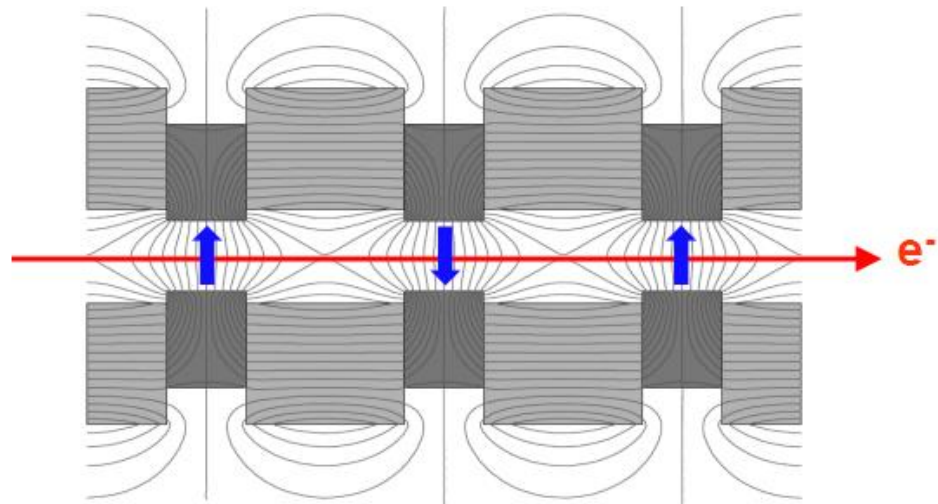
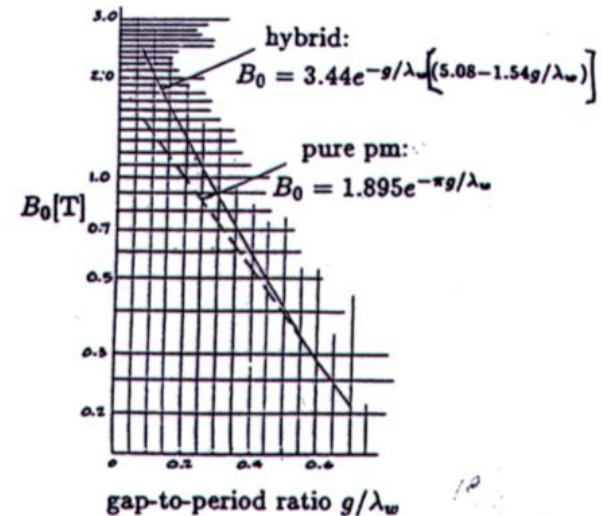- Pure structure magnet array

$$B_0[T] = 1.895(e^{-\pi g}/\lambda_u)$$

- Hybrid structure magnet array

  ➢ samarium-cobalt magnet

$$B_0[T] = 3.33 \exp\left[-\frac{g}{\lambda_u}\left(5.47 - 1.8\frac{g}{\lambda_u}\right)\right]$$

$$0.07 < \frac{g}{\lambda_u} < 0.7$$

  ➢ Neodymium-iron boron magnet

$$B_0[T] = 3.44 \exp\left[-\frac{g}{\lambda_u}\left[5.08 - 1.54\frac{g}{\lambda_u}\right]\right] \quad 0.085 < \frac{g}{\lambda_u} < 0.8$$

hybrid:
$B_0 = 3.44 e^{-g/\lambda_w}\left[5.08 - 1.54 g/\lambda_w\right]$

pure pm:
$B_0 = 1.895 e^{-\pi g/\lambda_w}$

gap-to-period ratio g/λ_w

Attainable on-axis field in pure PM and hybrid insertion devices (B_r = 1.1 T, H_{pm} = -0.8H_c)
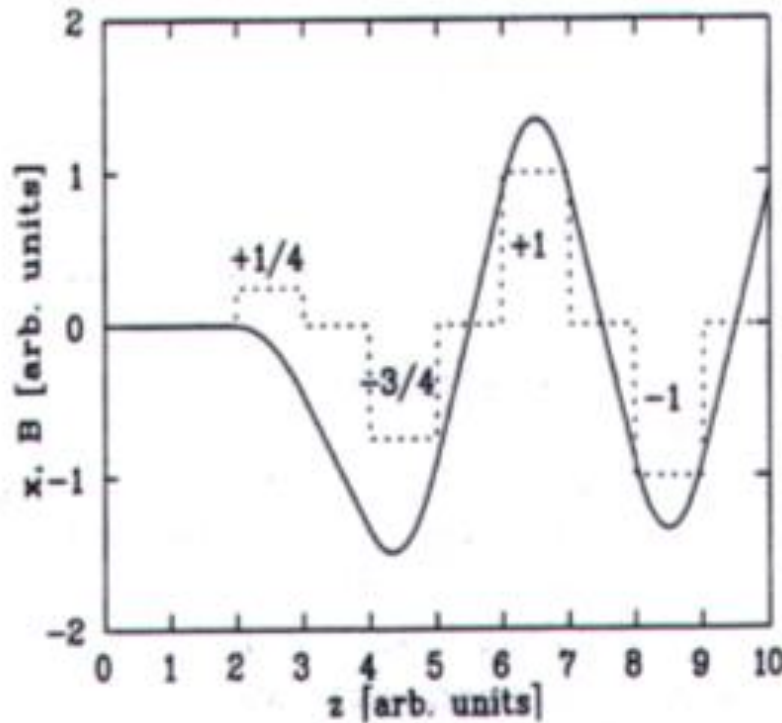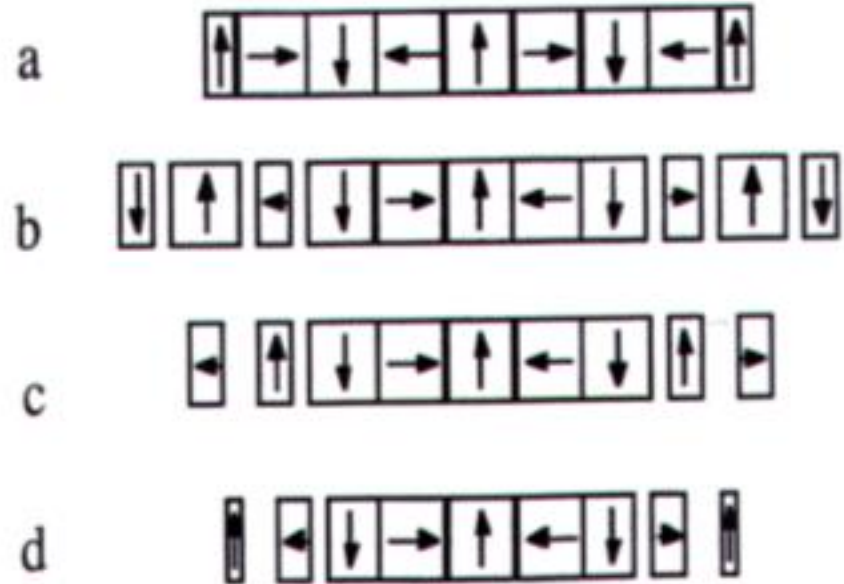
Design criteria of IDs

◆ **Wedged-poles** were shaped with a thicker cross section at pole tip.

◆ **Chamfers** are used to reduce local saturation and demagnetizing field

◆ **Vertical recess** to minimize on-axis field strength variation.

◆ **Magnet overhang** reduces 3-D leakage flux and roll-off is slower.

◆ **Different thickness of magnet block sizes** with partial strength on the both end poles.

◆ **0.5 mm thickness shim** at magnet edge increase vertical field roll-off.

◆ Two **rows of trim magnets** for B_y and B_x multipole field shimming.

◆ **Magnet & iron shim pieces** for trajectory and spectrum phase shimming.

◆ **Longitudinal distance** between each end pole, the **pole height**, and **pole tilt** can be adjustable.
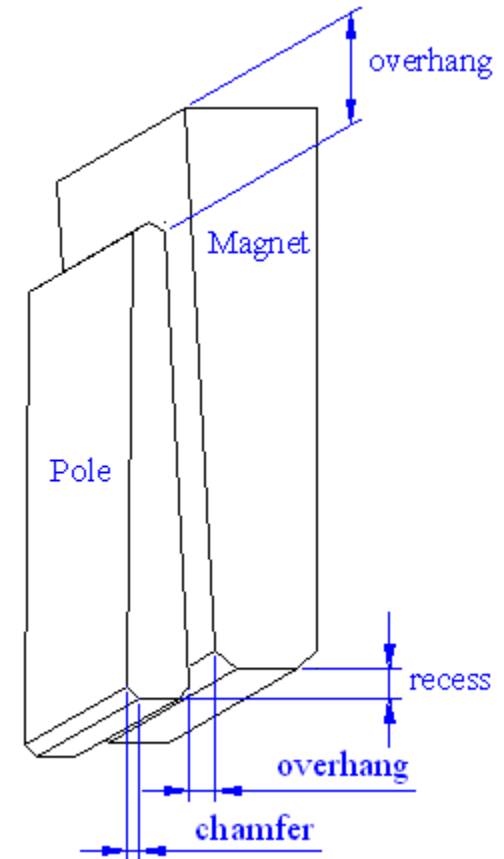
Sequence of magnet poles (dotted line) resulting in no offset between the electron trajectory (solid line) and the magnet axis.
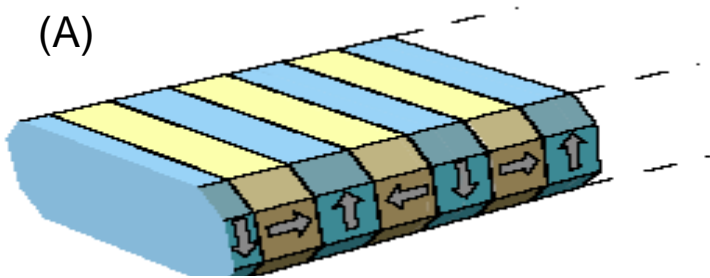
Various end-sequences for the pure-permanent magnet structure

The criteria of ID design:
1. First integral field ∫Bds=0
2. Second integral field ∫(∫ Bds')ds=0
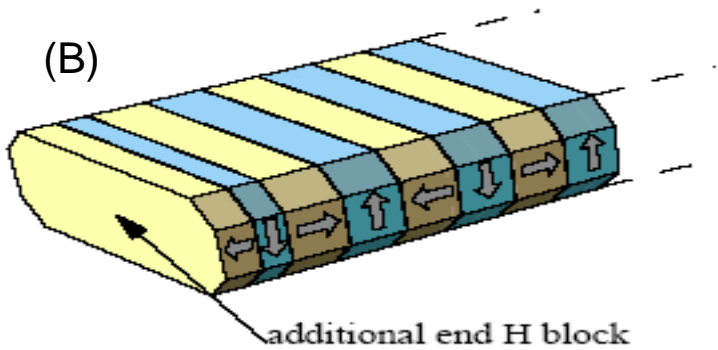
52

(A)

(B)

additional end H block

Reduce integral field strength with gap

(C)

blocks with tilted magnetization

Reduce integral field strength with gap and phase

53

J. Chavanne, C. Penel and P. Elleaume, Synchrotron Radiation News, 22, No. 4, 34 (2009).

Apple II End pole design

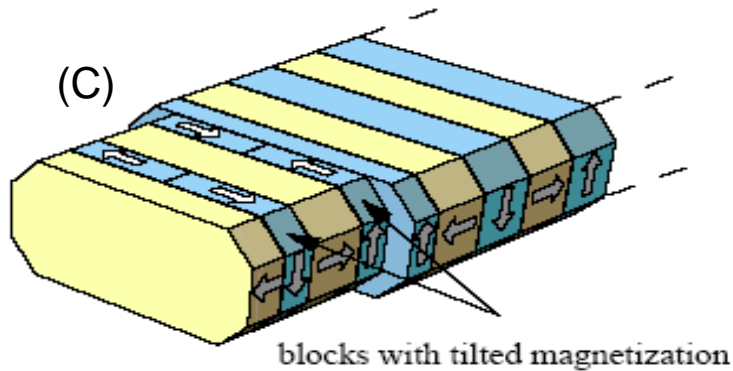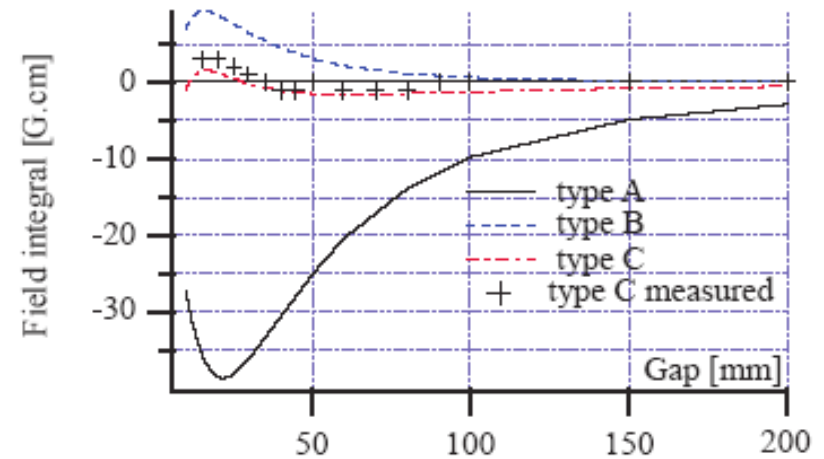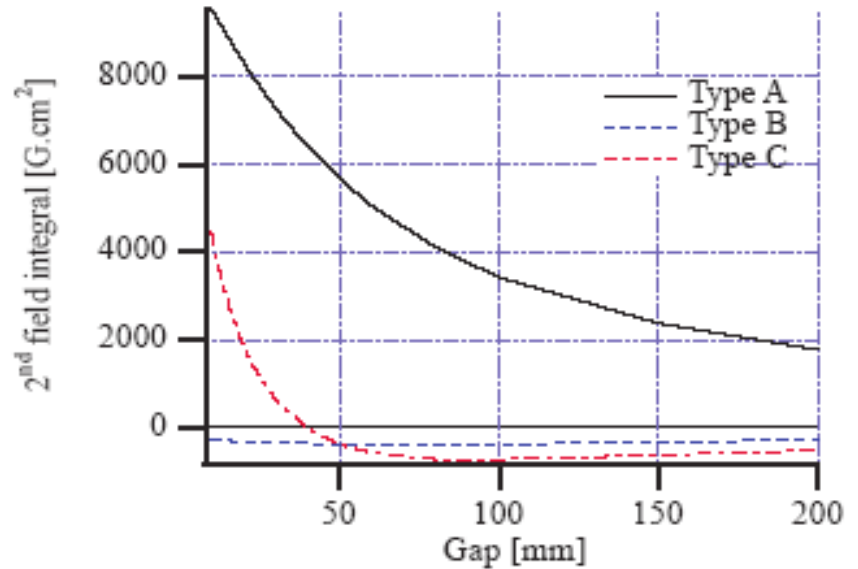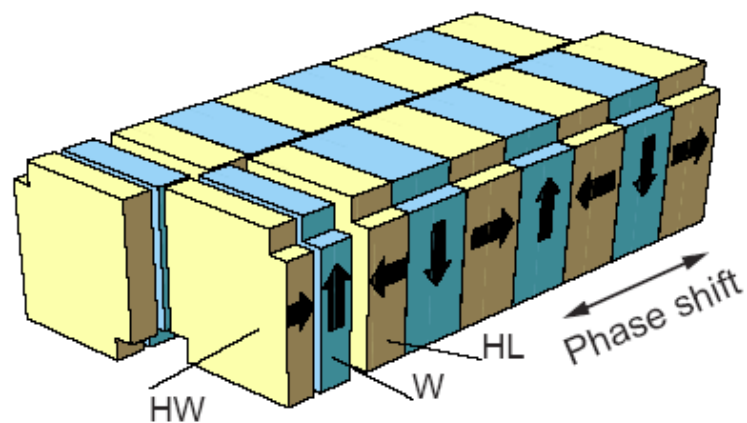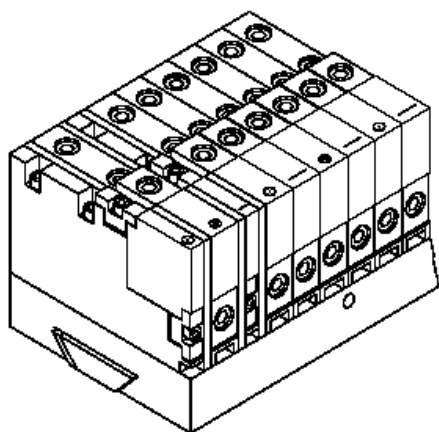The magnets of type HL, W and HW have the same cross-section but a different longitudinal dimension. The air gap is 5 mm (2 mm) between the HL and W (W and HW) magnet blocks.
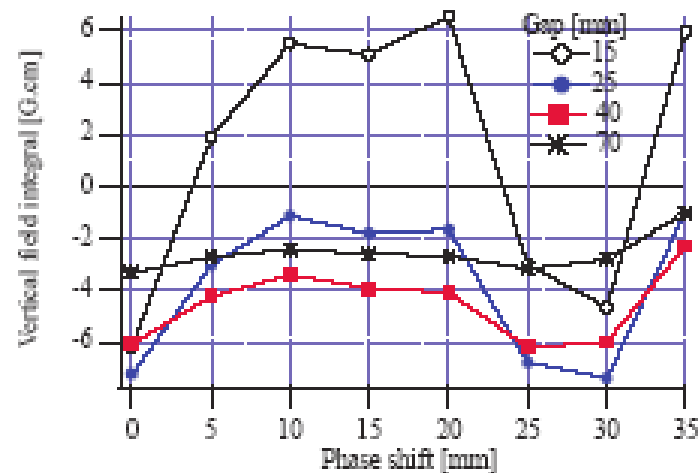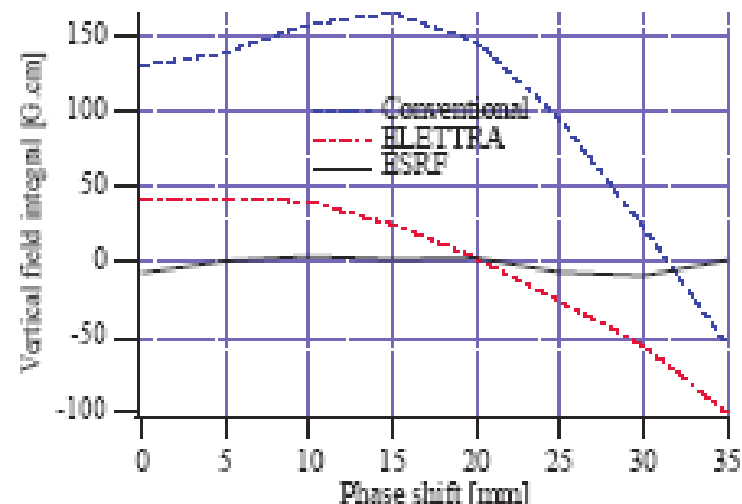
Reduce integral field strength with gap and phase & the second field integral

54

J. Chavanne, C. Penel and P. Elleaume, Synchrotron Radiation News, 22, No. 4, 34 (2009).

$$\Theta(z) = \frac{2\pi}{\lambda}\left(\frac{z}{2\gamma^2} - \frac{\int x'^2 \, dz}{2}\right)$$

where $x' = dx/dz$ represents the electron angle with respect to the undulator z-axis, λ is the photon radiation fundamental wavelength, and γ denotes the relativistic velocity. In the ideal undulator device, the phase at each pole should be a perfect linear variation and the phase error is zero.
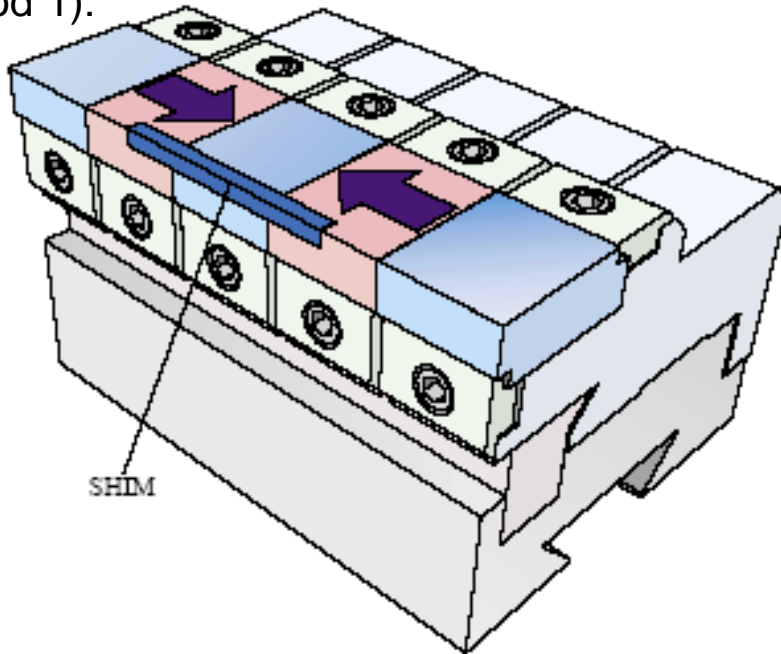
However for a real undulator, the phase error $\Delta\Theta$ is not zero and can be obtained by subtracting the two optimum linear fits of the real and ideal field

$$I = I_0 e^{-(n\Delta\Theta_{rms})^2}$$

Where I and I_0 represent the spectrum flux intensities with and without phase error.

Dynamic aperture shimming methods on EPU

(Method 1):

$$\int_{-\infty}^{\infty} \left(B_x + i\, B_y \right) dz \cong \sum_{n=0}^{n} \left(b_n + i\, a_n \right) \left(x + iy \right)^n.$$

Where a_n and b_n denote the integral normal and skew components.

The shimming method has been studied to re-enlarge the dynamic aperture with the addition of a multipole field component. Such shims are placed on each of the four magnet arrays. They are designed based on the criteria of correcting the tune shift vs. x.
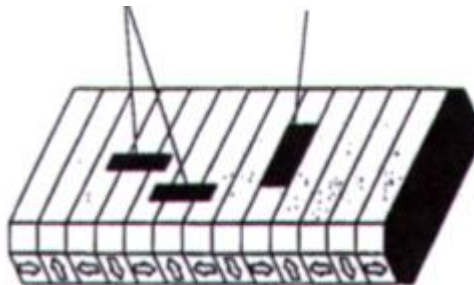
(Method 2):
Using multi filament flat wire on the surface of the EPU vacuum chamber to compensate for the multipole error which is induced from dynamic integral field.

56

J. Chavanne, et al., "Recent achievements and future prospect of ID activities at the ESRF", EPAC2000, 2346 (2000).
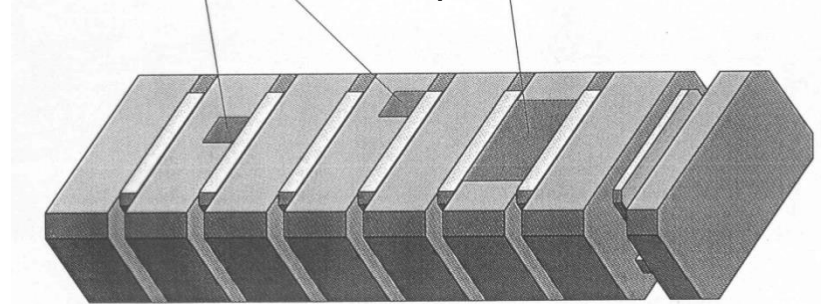
Multipole & spectrum shimming method

- Measuring the individual permanent magnet block and then arranging them by sorting block in the structure.

- Measuring the integral field strength of each block which on the keeper to reduce the mechanical error.

- Swapping blocks after assembly and field measurement.

- Using the thin iron pieces or permanent magnet pieces on magnet to correct the multipole and spectrum shimming.

Permanent magnet

Hybrid magnet

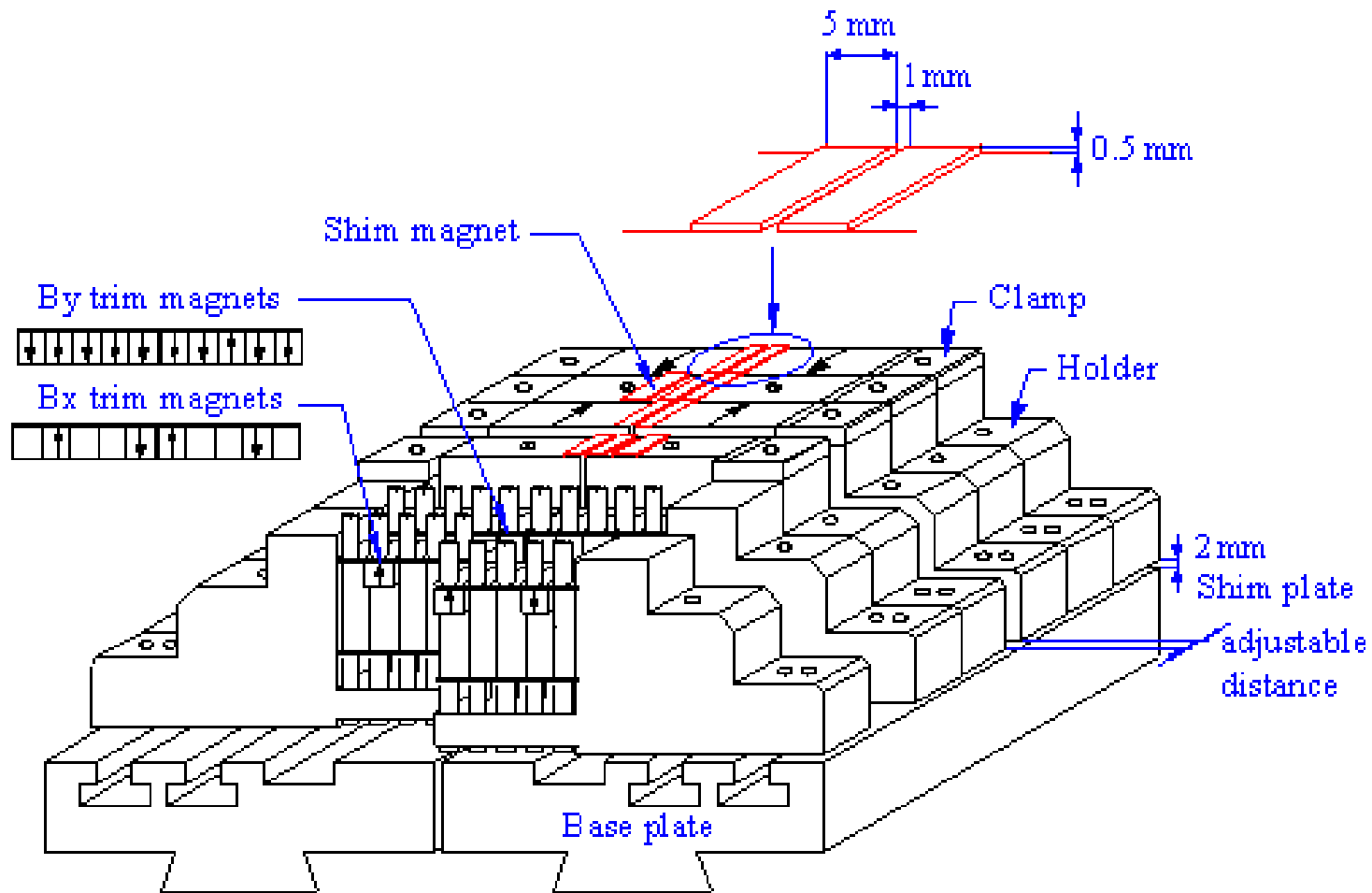Method of magnetic shimming to improve the magnetic field quality

57

J. Chavanne, et al., "Recent achievements and future prospect of ID activities at the ESRF", EPAC2000, 2346 (2000).

Field quality control by various methods

$$\int_{-\infty}^{\infty} \left(B_x + i\, B_y\right) dz \cong \sum_{n=0}^{n} \left(b_n + i\, a_n\right)\left(x + iy\right)^n.$$

Where a_n and b_n denote the integral normal and skew components.

58

參 考 書 目

1. Handbook of Accelerator Physics and Engineering, edited by Alexander Wu Chao and Maury Tigner, World Scentific (1998)
2. Accelerator Physics, S. Y. Lee, World Scientific Publishing Co. Pte. Ltd. (1999)
3. Synchrotron Radiation Sources: A Primer, H. Winick (ed.) (World Scientific, 1994)
4. Compact Synchrotron Light Sources, E. Weihreter (World Scientific, 1996)
5. An Introduction to Particle Accelerators, E.J.N. Wilson (Oxford Univ. Press, 2001)
6. Particle Accelerator Physics, 3rd ed., H. Wiedemann (Springer-Verlag, 2007)
7. The Physics of Particle Accelerators, K. Wille (Oxford Univ. Press, 2000)
8. . An Introduction to the Physics of High Energy Accelerators, D.A. Edwards & M.J. Syphers (Wiley, 1993)